日本沙漠学会誌

ISSN 0917-6985

VOL.10 NO.3 October 2000

沙漠研究

JOURNAL OF ARID LAND STUDIES

目　　次

日本沙漠学会

沙漠から世界へ ― 風送ダストプロジェクト―

気象研究所　三 上 正 男

沙漠を持たない国に住む我々日本人にとって，沙漠とは遙か彼方にある彼の地の事を指す．そのため我々が沙漠を思うとき，そこには何かしらロマンをかき立てるものがある．我々が沙漠に関わる研究を進めていく場合，個々人の内部的な推進力として，そういう要素は無視できない．さらに地球は一つであって，どんな地域であってもそれが独立には存在し得ないと言う抽象概念において，沙漠は世界に通じていると言う理解はあり得ても，具体的に日本の自然とどう関わるのかについて，個別具体的な研究は少なかったように思われる．すなわち従来の沙漠研究は，日本とはその社会的自然環境的成り立ちがまったく異なる沙漠の社会構造，自然環境を明らかにするための研究という側面が強かった．それはそれで科学として重要なことで，全ての普遍的認識は，個別特殊的な問題を一般化抽象化する事によって得られるからだ．しかし，一方において沙漠は世界に通じていると言う事実が存在する．抽象概念ではなくて具体的な物質「風送ダスト」を通じて．

このことを地球科学的手法により明らかにしようとする科学技術庁（振興調整費）の研究プロジェクトが始まった．プロジェクトの名称は「風送ダストの大気中への供給量評価と気候への影響に関する研究」というもので，日本と中国との共同研究として第一期３年間の計画で進められる．風送ダストは風送塵ともよばれる乾燥した地表面から風によって大気中に運ばれる鉱物質の微粒子のことを指す．これが大気中に浮遊した場合，鉱物質のエーロゾルとなって，大気の放射過程に大きな影響を及ぼすことが定性的には分かっている．一つは鉱物質の粒子が日射と長波放射の散乱及び吸収を引き起こす（直接的）効果である．また鉱物質エーロゾルは凝結核として雲・降水過程に関わっている（間接的効果）．大陸内陸部の沙漠地帯からは大量の風送ダストが大気中へ供給されており，実は大気中の重量比において鉱物質エーロゾルは全てのエーロゾル中の過半を占めている（IPCC第二次報告）．こうして大気中に大量に浮遊するダスト粒子は，やがて地球表面の７割を占める海洋へ沈着し，海洋表層の植物性プランクトンを涵養することが指摘されている．この過程は海洋の一次生産を通じ，全球の炭素循環に長い時間スケールで影響を与えていると考えられる．すなわち，砂漠地帯から舞い上がる風送ダストは，短い時間スケール（大気放射過程）と長い時間スケール（海洋一次生産過程）を通じて地球の気候維持形成に深く関わる因子であると考えられる．こうしたことは，これまで定性的に，あるいは簡単化した評価によってある程度定量的にも明らかにしようと試みられてきたが，その全貌の理解にまでは至っていない．

今回のプロジェクトは，その全過程を，地球物理学的手法による沙漠乾燥域の実態調査にふまえて，定量的に理解・評価しようとする試みである．このプロジェクトには，日本側から本学会会長の吉野正敏氏を始め多くの沙漠学会員が参加している．本プロジェクトの推進を通じて，日本沙漠学会の研究領域がさらに拡大する結果に繋がることを期待し，そのための努力も行いたいと思っている．今後様々な局面で学会会員諸氏の理解とご支援をお願いしたい．

沙漠研究 10-3, 171-181 (2000)
Journal of Arid Land Studies

— Review Article —

Problems in Climatology of Dust Storm and its Relation to Human Activities in Northwest China

YOSHINO Masatoshi*

This review paper deals with the recent works on dust storm climatology and the related human activities in Northwest China. Dust storms are grouped into four classes, which are defined in regard to wind velocity and visibility. The most severe class "extra-heavy", has a visibility of less than 50m and a maximum wind velocity of more than 25m/sec. Many monographs and collected papers on dust storms, desertification and related conditions have been published in the 1990's. From the standpoints of climatology, meteorology, geomorphology, geology, vegetation science and soil science, as well as human geography, some important results have been introduced in this paper. Studies on the status of the source region and the occurrence of dust storms in Xinjiang, the development and shifting of dust storm systems in the Hexi Corridor of Gansu, the movement and transport of dust and the spread of dust in East Asia are reviewed.

Human dimensions are of importance since wind damage results in higher amount of economic losses. In particular, these economic losses have been mone in La Niña years than in the El Niño years. For farmers in oases, increasing income is one of the most important means of decreasing or weakening the serious impact of dust storms in desertified areas, through reducing collection of firewood and increasing use of coal.

Key Words: Desertification, Dust storm, Kara-bran, Natural hazard, Wind damage

1. Introduction

Dust storms are one of the most important elements of the climate and environment in the arid regions of China. In particular, the occurrence of dust storms and their impact on human lives can be observed in every year (Yoshino, 1992, 1997). A review of the results of recent studies has led to a summary of problems caused by dust storms. This revised, expanded paper was read at the "Third Symposium on Aeolian Dust Originating from Arid and Semiarid Lands" held at the Institute of Physical and Chemical Research (RIKEN) on 24 September, 1998 (Yoshino, 1998).

The region under discussion and the names of mountain ranges, basins, deserts and oases, are shown in Fig. 1.

2. Definition of Dust Storm

The dust storm classification is as follows: "light": visibility is 500-1,000m and wind force is 4-5 (wind velocity is more than 10m/sec), "moderate": visibility is 500-1,000m but wind force is 6-7 (wind velocity is more than 17m/sec), "heavy": visibility is less than 500m and wind force is more than 8 (wind velocity is more than 20m/sec), and "extra-heavy": even though the definition differs according to provinces (regions), agencies (offices, departments) or researchers, it is generally visibility of less than 50m and maximum wind velocity of more than 25m/sec, or wind force of more than 10 (wind velocity is more than 22m/sec).

* Emeritus Professor, University Tsukuba. 5-1-8-202, Komazawa, Setagaya, Tokyo 154-0012, Japan.

(Received, May 27, 1999; Accepted, August 12, 1999)

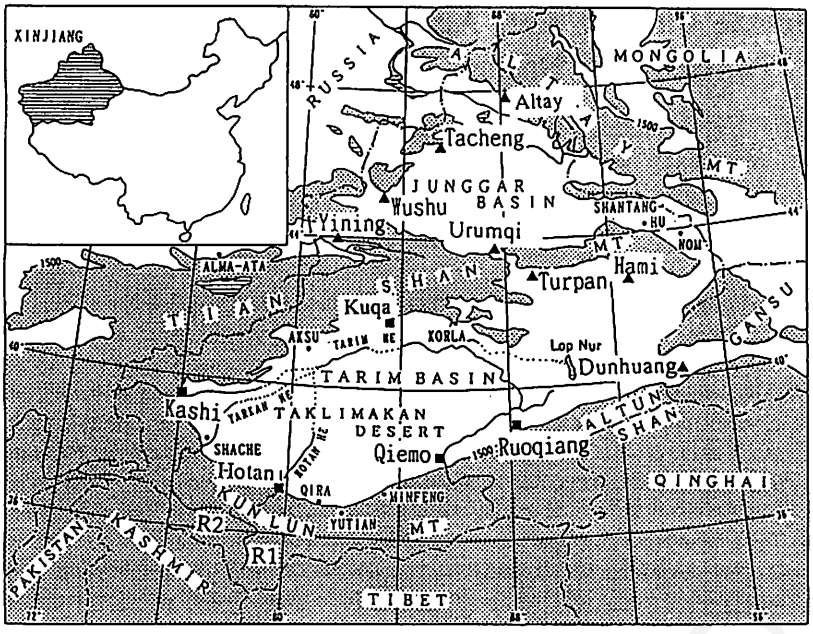

Fig. 1. Sketch map of the Xinjiang and part of the Gansu region, observation stations and oases.

3. Recent Studies

1) Monographs

A comprehensive monograph on "Kosa"(yellow sand) was published in Japanese in the early 1990's (Nagoya University, Research Institute for Hydrosphere, 1991). It contained chapters dealing with dust storm transport. Xia and Yang (1996) published a comprehensive monograph on dust storm damage and countermeasures in the northwestern parts of China. The authors concluded that factors such as overdevelopment, heavy deforestation, destruction of vegetation, overgrazing, inadequate use of water resources, changes in drainage patterns, intensification of the deterioration of vegetation and wind erosion due to drainage pattern changes, construction of transportation networks such as railways and roads, changes in ground surfaces to produce oil and mineral resources have been contributing to the development and increased occurrence of dust storms (Chao, 1984). Details will be mentioned later in the respective chapter.

Fang *et al.* (1997) published a volume of collected papers of studies on sand and dust storms in China. It contains many new results of recent studies, which will be separately cited later.

In a monograph on desertification in China, Yoshino (1997) dealt climatologically with the occurrences of dust storms and the impact on/by human activities, in particular agricultural land use in the oases.

In a monograph on the Quaternary glacier and environmental research in West China (Chinese Research Center for Quaternary Glacier and Environment, and Chinese Committee on Quaternary Research, 1991), much information was presented regarding paleoclimates and paleoenvironments, including 39 papers on dust fall, paleo-aeolian and depositions, mainly from the geological point of view.

Chen *et al.* (1998) summarized the studies on aeolian sandy soils in the arid regions of China developed by wind-formed sandy parent materials. Such soils generally have a sandy layer 1 meter or more in thickness, mainly consisting of well-sorted fine sand. It was noted that the classification of soil groups under the sandy entisol suborder must consider differences in moisture and temperature regimes; in other words, the moisture and temperature regions can be used as a basis for their soil group classification. They emphasized the importance of the utilization of the aeolian sandy soils for consideration

together with amelioration and protection.

Wu *et al.* (1997) published a volume of collected papers of his research since the 1960's on sand movement, aeolian landforms, and sand-driving wind. In particular, his studies were of importance from a geomorphological approach on the development of sand deserts in the Zhungger Basin. It was shown that the winds in April, May, September and October are the most influential in the processes of sand dune movement and formation.

Agricultural ecosystems of deserts and oases were studied intensively by Li *et al.* (1998). The direct impact of dust storms on the ecosystem was not dealt with, but the results of the studies contribute to a basic consideration of the rational utilization of water resources and the advancement of land degradation/desertification. For example, the area of grassland in Xinjiang is 572,670km^2, which comprises 34.4% of the total area, but it has been decreasing very rapidly during recent years. In other words, dust storm occurrence and the degree of severity are rapidly increasing.

2) Synthesis papers

There are many review papers on climate change, environmental change, desertification and the impact on/of human activities in the arid and semi-arid regions in China, but few on dust storms, except for the papers in the monograph by Fang *et al.* (1997) mentioned above. In this sectoion, several papers on general views written in English are introduced. Zhao (1996) contributed a paper dealing with climate change and sustainable development. He pointed out the decrease of the annual mean wind speed by 0.2-2m/sec and the decrease of the number of days with strong winds by 3-35 days per year over the period between the 1950's and the 1970's. It was thought that these decreases might be caused by natural climate changes, the building of shelter belts and urbanization surrounding observation stations.

The working group on "Operational Use of Climatological Knowledge" by the Commission Climate (CCL) of the WMO discussed the importance of studies on water resources, drought and desertification in China (Li, 1996). It was shown that the estimated glacier change (decrease) in the past 500 years in Northwest China was 35% in Altay, 25% in Tienshan, 23% in Pamir, 11% in Karakorum and Kunlun, and 40% in Qiling. The Intergovernmental Panel on Climate Change (IPCC) included a summary of land degradation and desertification, but did not deal with the effect of dust storms. Regarding wind erosion effects in arid and semi-arid regions, it was written that climate change in the coming century is expected to lead to more droughty soils and less vegetation due to higher evaporation rates (Bullock and Le Houérou, 1996). Consequently, it is considered that wind erosion and dust storm occurrence may become more frequent.

The book, "Regional Geography of Xinjiang", Volume 10, was dedicated to a comprehensive climatography (Xinjiang Uygur Zizhiqu, Regional Geography Editorial Committee *et al.*, 1995). The chapter on meteorological disasters described the details of strong windstorms and sandstorms. It was pointed out that sandstorms are the most frequent in the northern and southeastern parts of the Tarim Basin and occur for 90-110 days. In the western part, they occur for 40-80 days, and in the remaining parts for 15-30 days. The book chronologically described occurrences of serious wind damage since 1761.

4. Dust Storms of the Past

1) Postglacial period

In the last 20,000 years, six stages of terrace formation have been distinguished along the Keriya River (Kanemaki *et al.*, 1994; Endo *et al.*, 1995, 1997). They occurred 16,700, 13,500, 10,000-9,500, 6,500-5,400 and 1,600 years ago (Chao and Xia, 1992) and in recent years (Zhu, 1984). It was assumed that aeolian activity, such as sand-dune formation, was dominant between these periods due to drier and warmer climate conditions. From their figure (Fig. 8 of Kanemaki *et al.*, 1994), the peaks of sand-dune periods can be interpreted as having occurred 15,600, 12,500, 8,000, 4,300, and 800 years ago. Precisely speaking, aeolian activity may not correspond to dust storm activity (frequency, intensity in time and space, *etc.*), but we should pay attention to these variations during the postglacial period. Furthermore, based on these analyses, Endo *et al.* (1997) reported that the Holocene environment was extremely arid, particularly in the last 1,500 years. If this tendency continues, we should be cautious of increasing dust storm activity in the coming century.

The origin and routes of aeolian dust quartz were

studied by assuming that the values of the election spin resonance (ESR) signal intensity reflect those of quartz in areas along their routes (Ono, 1998; Ono *et al.*, 1998). It was pointed out that the northern limit of their distribution in North Japan corresponds to the position of the subtropical westerly jet stream in summer, and the southern limit to the position of the subtropical jet stream in winter. It is very interesting to note that because dust transport occurs mainly in spring, "the transitional season" between winter and summer, aeolian quartz distribution boundaries show a rough correspondence to the latitudinal shifting of the axis of the jet stream on a geological time scale. In my opinion, however, these are positional correspondences and this does not mean that the quartz is transported by the jet stream directly. Quartz is transported by meteorological systems in the lower troposphere under the influence of the upper level jet streams, even on a paleoenvironmental time scale.

2) Historical period

In China, dust fall phenomena have been called "yüdu" or "yümei" and reported since around A.D. 300 (Zhang, 1982). The highest frequency of these dust falls was occurred in April reaching 26% of the total cases. March, February and May then followed. Secular changes reveal that dust fall frequencies in North/East China had three predominant peaks around A.D. 1180-1300, 1500-1710, and 1800-1880. On the other hand, the periods of less frequency of floods were occurred at A.D. 150-650, 1120-1280 and 1680-1880, which imply drier and colder periods (Fang, 1990). Therefore, it can be concluded that dust falls were frequent in the colder periods, due to the drier climatic conditions and strong cold air flows from the Siberian anticyclone (Zhang, 1984; Fang, 1990). The dust fall frequency since the 15 century is given in Fig. 2, which clearly indicates opposite tendencies between the temperature and dust fall frequency during the recent historical period (Zhang, 1982).

This correspondence of the dust fall frequency and dry-cold (wet-warm) periods in a historical period is different from the tendency of sand-dune formation in the post-glacial periods mentioned above. The reason why they differ can be attributed to the different time scales (geological and historical) and to the different regions (Tarim Basin and North/East China).

5. Dust Storm Climatology

1) Distribution and recent changes of occurrence

According to a statistical report for the period 1949-1990 (Editorial Committee "Mitigation of Natural Hazard in Xinjiang for 40 Years", 1993), wind damage occurred a total of 195 times, 108 deaths, 46,000 dead animals, 4,000 damaged houses, and a total economic loss of 2,260,000 Chinese Yuan. These totals are ranked number three for flood and hail damage in Xinjiang.

Dust storm distributions can be interpreted from the distribution of wind damage, as shown in Fig. 3. The most frequently affected regions are located in the Turpan and Hami regions in the east and in the area surrounding Altay in the north. In the Taklimakan desert, the northern part is more frequently affected than

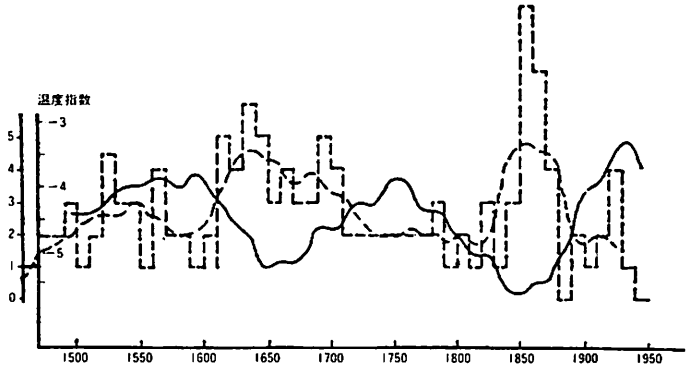

Fig. 2. Secular changes in the frequency of dust fall (histo-gram), its 5-year-running mean (broken line), and temperature index (solid line) (Zhang, 1982).

the southern part. Such patterns are different from the distributions of the number of days with strong wind and the observed maximum records (Yoshino, 1992).

The recent change in the amount of area damaged by wind is striking. During the last 80 years, the area has increased logarithmically, as shown in Fig. 4. In particular, a tremendous increase was seen in the second half of the 1980's.

The total frequencies of "heavy" and "extra-heavy" dust storms were 5 in the 1950's, 8 in the 1960's, 13 in the 1970's, 14 in the 1980's and 8 in the first half of the 1990's. During the last 40 years, climate in oases has been changing (Du, 1993a, b) and the frequency of dust storm is also changing.

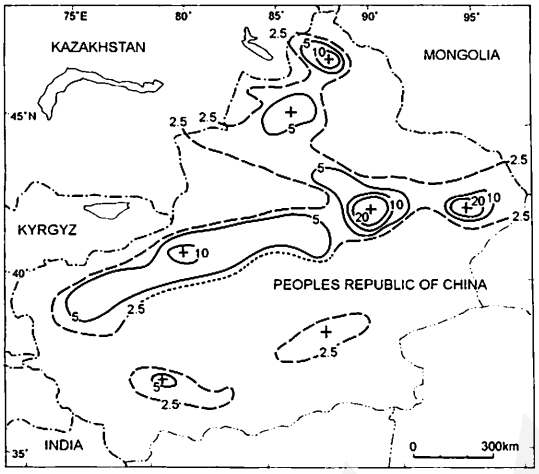

Fig. 3. Distribution of frequency of wind damage in Xinjiang, 1949-1990.

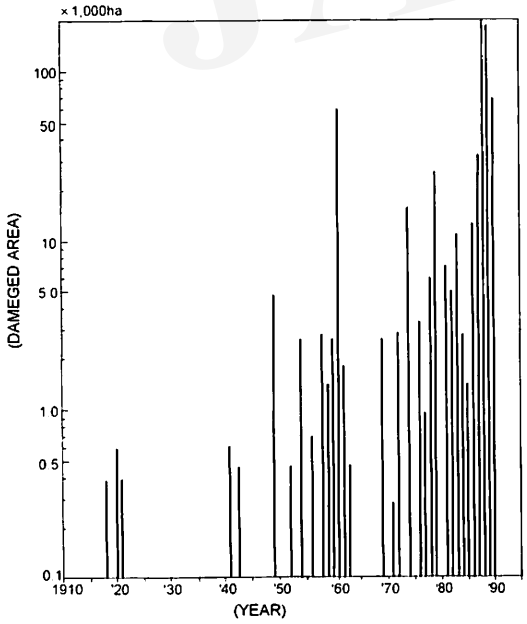

Fig. 4. Trend of change in wind damage area (1,000ha) in Xinjiang, 1910-1990.

2) Seasonal and diurnal variation

The monthly change in the frequency of "heavy" and "extra-heavy" dust storms observed in Northwest China is given in Fig. 5 (Qian *et al.*, 1997). They occur most frequently in April, followed by May and March. This is the spring season, in which the atmospheric circulation changes from a winter pattern to a summer pattern; in other words, cold air invades the upper layer of the troposphere relatively easily and the ground surface temperature increases. This results in stronger convection of the air with cold-front movement. In an extreme case, it causes observable severe dust storm movement with cold front shifting as mentioned later in section 6-2) again.

Diurnal variations in the frequency of "heavy" and "extra-heavy" sand and dust storms at Minfeng and Hotan during the period of 1952-1992 are shown in Fig. 6. These variations occur most frequently in the hours 15-16 by Beijing time. Since longitudinal differences between Beijing and these weather stations are 30-35 degrees, it can be said that they occur in most cases, in hours of 13-14 by local time. The reason why the diurnal variations occur most frequently in the early afternoon can be attributed to the effect of convectional activities caused by the most unstable conditions of the atmosphere due to the warmed ground surface.

3) Main routes and dust storm regions

The main routes of dust storm movement and the regional division according to the frequency of occur-

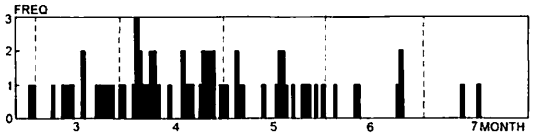

Fig. 5. Monthly change in the number of days with "heavy" and "extra-heavy" sand and dust storms in Northwest China, total between 1952-1992 (Qian *et al.*, 1997).

rence are given in Fig. 7 (Xu and Ho, 1997). The highest frequency is seen from the Hami region to the Yuilin region of the Ordos through the Hexi Corridor of Gansu. The northwestern route has the most frequent occurrence of dust storms (76.9%). The western route is next (15.4%). The frequency for route from the north is low (7.7%) (Xu and Ho, 1997). The main routes represented by thick black lines show the influence of the Tienshan Mountain Range. The region with the highest frequency corresponds to the driest region with an annual precipitation of less than 100mm.

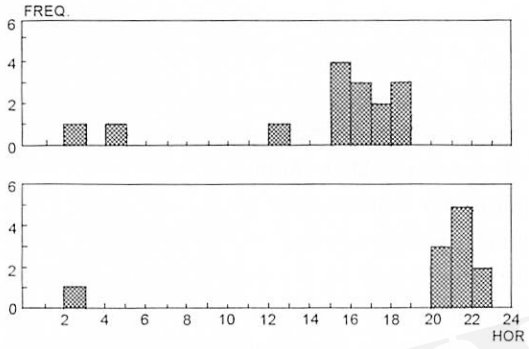

Fig. 6. Diurnal fluctuation of set-in time of "heavy" and "extra-heavy" sand and dust storm occurrence at Minfeng (upper figure) and at Hotan (lower figure), 1952-1992 (Qian *et al.*, 1997).

6. Meteorological Analysis of Dust Storm

1) Origin and routes

Present-day aeolian dust in Japan is called "Kosa" (yellow sand), although the grain size is finer than silt. Its origin and routes have been studied by tracing back the trajectory of dust clouds using satellite images (Chung, 1986). Kai *et al.* (1988, 1998) studied dust transport from the source region to the Asia and Pacific region from 8 to 13 May 1986. It took 5-6 days for dust to be transported from the Taklimakan desert area and 2-3 days from the Loess Plateau area to the upper tropospheric layer over Japan. It was shown that "the dust" spread up-wards and meridionally in accordance with the duration of transport.

These analyses are very important for understanding the present-day impact of dust storms on atmospheric and ground conditions and on human society, but also for interpreting the phenomena in historical and geological times.

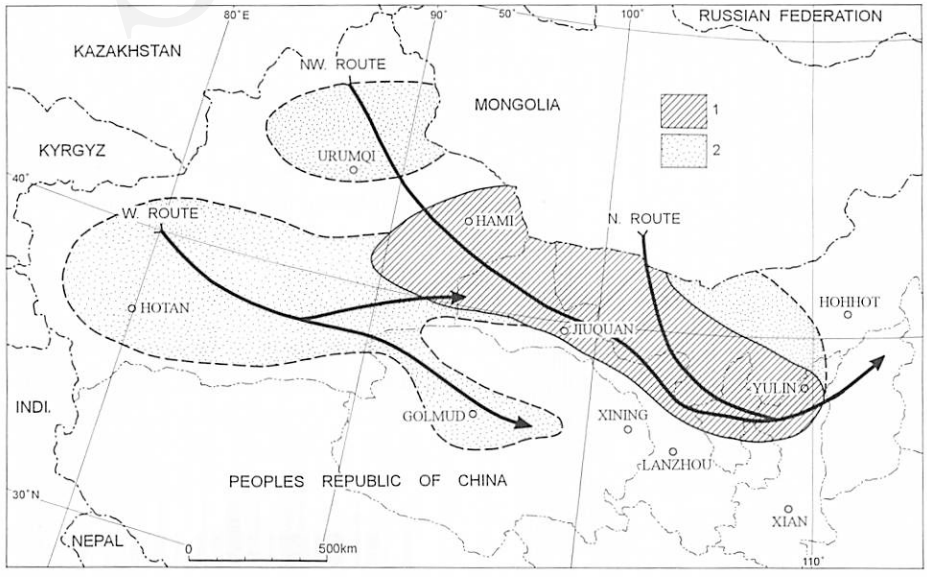

Fig. 7. Main routes and regional divisions of sand and dust storms in Northwest China.
1: The region where the heavy sand and dust storms occur most frequently.
2: The region where they occur frequently (Xu and Ho, 1997).

2) Some case studies

On 22 April 1977, there occurred one of the most severe Kara-bran (means "black wind", violent dust storm) in the Hexi Corridor of Gansu, with an instantaneous wind velocity higher than 25m/sec and visibility less than 50m. Many weather stations observed a mean wind velocity of more than wind force 12. The duration of a wind force of more than 8 was about 2 hours at many stations and, at the station with the worst conditions, it continued for 5 hours.

The synoptic weather situation was that a low-pressure area over Siberia had constantly moved eastward since 19 April. On 22 April, the trough arrived at the northern part of Xinjiang. A maximum drop in air temperature was seen at the 700hPa level in the southern part of Xinjiang. A cold anticyclone was formed in the western part of South Xinjiang. Behind the cold front, a Kara-bran area with a width of about 400km developed. Its upper boundry was about 1,000m. Within 10 minutes after the arrival of the Kara-bran, air pressure increased 2.8hPa, air temperature decreased 6.8℃, and the wind direction changed to WNW (Bai and Xu, 1991). An analysis on the long-range dust transport in association with jet stream was made for the case on 17-18 April, 1980 (Liu *et al.*, 1981, 1985). It was indicated that dust raised by strong turbulent mixing ahead of advancing cold front in the deserts of Northwest China was carried rapidly eastwards, as shown in Fig. 8. In addition, surface wind-speeds and turbulence were intensified by a down-ward transfer of momentum from the upper westerlies (Pye, 1987).

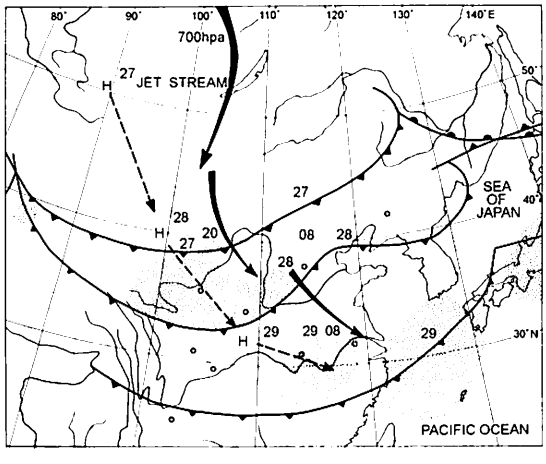

Fig. 8. Movement of dust storm region and cold front on 27-29 April 1983 (Zheng and Chao, 1997).

These changes were more than those occurring during a normal cold front, and resulted in very sharp up and down air motion as well as an observable horizontal temperature gradient of more than 10℃/100km.

The criteria for the short-range weather prediction of wind/dust storms are an air temperature difference ΔT (Tazhong-Hotan) of -11.1℃ at the 700hPa level at 8:00AM and an air pressure difference ΔP of -4.4hPa in spring (March to May) with differences of -9.4℃ and -2.3hPa in summer (June to August) (Editorial Group "Guidebook of Short-Range Weather Forecasting in Xinjiang", 1987).

7. Human Dimensions

1) Human activities and dust storms

Between the desertification and the occurrence of dust storms, there are always processes of human activities. These processes have two opposing effects. For example, sand-dune invasions into oases, wind and dust storm occurrences, the expansion of regions with wind damage, and the abandonment of oases due to decreasing water resources for irrigation and drinking are the results of the impact on and, at the same time, of human activities. Yoshino (1995) reported the relationship between human activities and disaster in Taklimakan Desert. Soma (1996) discussed the effect of salinization on desertification partly caused by wind erosion. Furthermore, it should be stressed that damages by sand and dust storms in 1990's become more and more severe and frequent for human society (Sun and Huang, 1998).

Table 1 shows the natural hazards occurring in Xinjiang during the period of 1949-1990. As mentioned in Section 5-1), the occurrence and total cost of wind damage are high among the various natural hazards.

There is a clear difference in wind damage between the El Niño and La Niña years. Taking the examples of 1977, 1982 and 1987 as the El Niño years and 1975, 1988 and 1989 as the La Niña years, respective mean values were calculated as shown in Table 2. In the La Niña years, livestock loss was 8 times more than that in the El Niño years and this contributed to the tremendous economic loss due to damage in the La Niña years. Crop yields and transportation also suffered from wind damage. This damage occurred because of the development of sand

Table 1 Natural hazards in Xinjiang, 1949-1990.

	Number of cases of occurrence	Loss		Number of houses destroyed	Total cost of damage
		People	Livestock		
		head	×1,000	×1,000	× million US$
Earthquake	32	125	101	41	24.5
Drought	58	0	156	0	12.3
Flood	498	1,523	255	98	63.3
Wind damage	195	108	46	4	24.9
Hail damage	403	56	76	6	40.3
Cold wave & frost damage	217	212	7,773	2	6.1
Thunderstorm	19	15	0	0	0.0
Insects and desease	80	4	0	0	5.6
Fire	24	12	0	1	0.8
Total	1,526	2,055	8,407	152	177.8

Table 2 Wind damage and drought in Xinjiang in the El Niño and La Niña years.

	Total cases per year	Loss		Number of hauses destroyed	Total cost of damage
		People	Livestocks		
Wind damage					
El Niño year	5.7	2.0	923	699	8.7 ×mill USD
La Niña year	7.5	0.3	7,234	432	1,890.9
Drought					
El Niño year	3.0	0.0	1,038	0	2.5
La Niña year	4.0	0.0	8,000	0	4,101.8

and dust storms caused by weather processes under the influence of the atmospheric circulation of the La Niña situation. In contrast, however, a recent study (Zhu and Zuang, 1998) reported that severe dust storms in 1952, 1977, 1983 and 1993 occurred in El Niño years. Further study is needed.

In China, there are studies on the history of population since the 1st century B.C. Also, centuries-total dust storm frequency has been reconstructed. Taking these values, the relationship between them was obtained as shown in Fig. 9. It seems that their absolute values are still to be studied, but Fig. 9 shows a good relationship between them, as far as the period until the 20th century concerned (Yoshino, 1995).

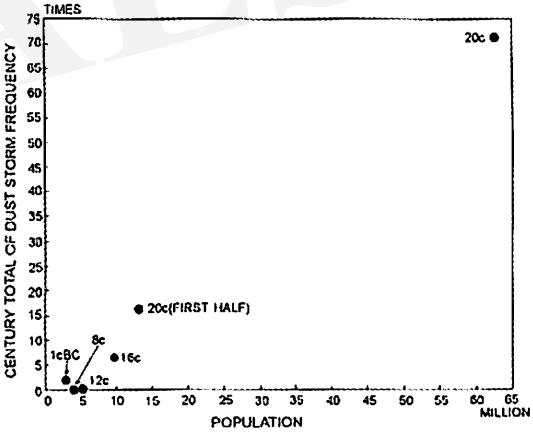

Fig. 9. Relationship between total (century) frequency of dust storms and population in the northwestern part of China.

2) Farmers and dust storms

The 98-99% farmers are Uygur, where as Han people work in industry, commerce, and other sectors of the service industry. The farmers must go into the desert to collect firewood, if they do not earn enough money to buy coal (15-17 US Dollar/ton and they use 1-2ton/winter season), through working on the side, for example, carpet production mainly by the women in the family.

During the early 1990's, about 10% of farmers' families in the oases on the southern fringe of the Taklimakan desert used coal. In the oases on the northern and western fringes, almost 100% of the farmers' families used coal, 20% of which went to the desert 7-10 times per winter to collect firewood in order to reduce spending (Yoshino *et al.*, 1996).

The GDP of farmers in the southern to southeastern regions of the Taklimakan desert is lower than those in the northern and western regions. For example, the rate of increase of agricultural production per person in the northern and western oases from 1985 to 1991 was 2.7-3.2 times higher than those in the southern oases (Du *et al.*, 1996).

It is pointed out that increasing the income of farmers is one important means of decreasing or weakening the serious impact of dust storms in desertified areas. The incidence of collecting firewood can be reduced, by improving the economic conditions for the farmers' families (Yoshino, 1997).

8. Conclusion

Comprehensive monographs related to dust storms and their impact on human activities published in the 1990's were first reviewed. In particular, it is interesting to note that they concentrate on the last 2-3 years. Secondly, review papers or synthesis papers were introduced to summarize the problems. Dust storms in the postglacial, historical and present periods were dealt with. There is a significant relationship between the frequency of occurrence and population. It was also shown that the fluctuation and changing pattern of dust storms are different according to the time scale. Seasonally speaking, sand and dust storms are concentrated in April followed by May and March. The diurnal variation is interesting; heavy and extra-heavy dust storms develop to most strongly afternoon to early evening.

There are three main routes of dust storms in Northwest China. It was indicated that dust from the source areas to East Asia takes 5-6 days in the case of the Taklimakan desert and 2-3 days in the case of the Loess Plateau. Furthermore, cold air mass invasion at the ground level is closely related to the areas with severe dust storms.

Human dimensions, as interpreted from the amount and frequency of wind damage, are of importance. They are highest among the various natural hazards. Wind damage was more serious in the La Niña years. In particular, loss of livestock due to strong sand and dust storms was about eight times higher in the La Niña years than in the El Niño years. For the farmers in oases, an increase in income is one important means of decreasing or weakening the serious impact of dust storms in desertified areas.

References

Bai, Zhaohua and Xu, Guochang (1991): *Weather of Northwest China*. Meteorology Press, Beijing, 443 p. (in Chinese)

Bullock, P. and Le Houérou, H. (1996): Land degradation and desertification. *In* Watson, R.T., Zinyowera, M.C. and Moss, R.H. eds., *Climate Changes 1955. Impacts, Adaptations and Mitigation of Climate Change: Scientific-Technical Analyses*, WG II, SAR of IPCC, Cambridge University Press, Cambridge, 171-189.

Chao, Sungchiao (1984): The sandy deserts and the Gobi of China. *In* El-Baz, F. ed., *Deserts and Arid Lands*, Martinus Nijhoff Publ. The Hague, 95-113.

Chao, Q. and Xia, X. (1992): A preliminary study on geomorphology and Quaternary geology in the lower reaches of the Keriya River. *Scientia Geographica Sinica*, 12: 34-43.

Chen, Longhang, Li, Fuxing, Di, Xingmin and Zhang, Jixian (1998) : *Aeolian Sandy Soils in China*. Science Press, Beijing, China, 188p. (in Chinese with English abstract)

Chinese Research Center for Quaternary Glacier and Environment and Chinese Committee on Quaternary Research (1991): *The Quaternary Glacier and Environment of Western China*. Science Press, Beijing, 330p.

Chung, Y.S. (1986): Air pollution detection by satellites; The transport and deposition of air pollutants over oceans. *Atmos. Environ.*, 20: 617-630.

Du, Mingyuan (1993a): Variations in air temperature and precipitation in arid areas of China in recent 40 years. *Abstr. 1993 Ann Meeting, Japanese Ass. for Arid Land Studies, 4*, 5-6.

Du, Mingyuan (1993b): Is it a global change impact that the climate is becoming better in the western part of the arid region of China? *Theor. Appl. Climatology*, 55: 139-150.

Du, Mingyuan, Yoshino, M., Fujita, Y., Arizono, S., Maki, T. and Lei, J.-q. (1996): Climate change and agricultural activities in the Taklimakan Desert, China, in recent years. *J. Arid Land Studies*, 5: 173-183.

Editorial Committee "Mitigation of Natural Hazard in Xinjiang for 40 Years." (1993): *Mitigation of Natural Hazard in Xinjiang for 40 years*. Earthquake Press, Beijing, 312 p. (in Chinese)

Editorial Group, "Guidebook of Short-Range Weather Forecasting in Xinjiang." (1987): *Guidebook of Short-range Weather Forecasting*. Xinjiang Peoples' Press, Ürümqi, 457p. (in Chinese)

Endo, K., Kanemaki, M., Watanabe, M., Ono, Y., Sohma, H., Zhao, Y.-j. and Mu, G. (1995): Environmental changes in and

around Taklimakan desert and the surrounding areas. *Proc. Intern. Symp. "Paleoenvironmental Change in Tropical-Subtropical Monsoon Asia", Special Publ., 24*, 177-187.

Endo, K., Yan, S., Kanemaki, M., Sohma, H. and Mu, G. (1997): Evolution of paleoenvironments in Tarim Basin. *J. Geography (Chigaku Zasshi)*, **106**: 145-154. (in Japanese with English abstract)

Fang, Jinqi (1990): The impact of climatic change on the Chinese migrations in historical times. *"Global Change and Environmental Evolution in China". Proc. of Section 3, Regional Conference on Asian Pacific Countries of IGU, 1990*, 96-103.

Fang, Zongyou, Zhu, Fukang, Jiang, Jixi and Qian, Zhenan (1997): *Studies on Sand and Dust Storms in China*. Meteorology Press, Beijing, 158p. (in Chinese)

Kai, K., Okada, Y., Uchino, O., Tabata, I., Nakamura, H., Taguchi, T. and Nikaidou, Y. (1988): Lidar observation and numerical simulation of a Kosa (Asian Dust) over Tsukuba, Japan during the spring of 1986. *J. Meteorol. Soc. Japan*, **66**: 457-472.

Kai, K., Takasugi, T. and Naramura, H. (1998): Long-range transport of the Asian dust storm (Kosa) particles originated from the Takla Makan Desert. *J. Arid Land Studies*, **7**: 107-117.

Kanemaki, M., Endo, K., Xia, X., Cao, Q., Watanabe, M., Sohma, H., Mu, G., Zhao, Y., Zhou, X., Hamada, S. and Fujikawa, K. (1994): Last glacial-Holocene environments in Keriya river field, Taklimakan Desert. *Proc. of the Inst. of Natural Sciences, Nihon Univ., 30*, 75-86. (in Japanese with English abstract)

Li, Berang (1996): Water resources, drought and desertification. *Report of the 2nd Session of the CCL Working Group on Operational Use of Climatological Knowledge. WCASP-37, WMO/TD-No.774, World Meteorological Organization*, 21-31.

Li, Shugang, Cheng, Xinjun and Wang, Zhouqiong (1998): *Agricultural Ecosystems of Deserts and Oases*. Meteorology Press, Beijing, 138p. (in Chinese)

Liu, Tungsheng, Gu, Xiongfei, An, Zhisheng and Fan, Yongxian (1981): The dust fall in Beijing, China, on April 18, 1980. *Geol. Soc. Amer. Special Pap.*, **186**: 149-158.

Liu, Tungsheng, Chen, Mingyang and Li, Xiufang (1985): A satellite images study of the dust storm at Beijing on April 17-21, 1980. *In* Liu, T. ed., *Quaternary Geology and Environment of China*, Ocean Press, Beijing, 17-21. (in Chinese)

Nagoya University, Research Institute for Hydrosphere (1991): *Science of Atmosphere and Hydrosphere Sciences, Kosa*. Kokonshoin, Tokyo, 328p. (in Japanese)

Ono, Y. (1998): Reconstruction of last paleoenvironments and paleomonsoon changes in Eastern Asia. *Global Ernvironmental Change*, **1**(1/2): 35-42.

Ono, Y., Naruse, T., Ikeya, N., Kohno, H. and Toyoda, S. (1998): Origin and derived courses of eolian dust quartz deposited during marine isotope stage 2 in East Asia, suggested by ESR signal intensity. *Global and Planetary Change*, **18**: 129-135.

Pye, K. (1987): *Aeolian Dust and Dust Deposits*. Academic Press, London, 334p.

Qian, Zhengan, He, Huixia, Zhuo, Zhang and Zhang, Hinlian (1997): Standard classification, and occurrence chronology of sand and dust storms in the northwestern region of China. *In* Fang, Z.-y. *et al.* eds., *Studies on Sand and Dust Storms in China*, Meteorology Press, Beijing, 1-10. (in Chinese)

Soma, H. (1996): Desertification in the Taklimakan Desert: Salinization, expansion of sand-covered area and wind erosion. *J. Arid Land Studies*, **5**: 117-129. (in Japanese with English abstract)

Sun, Lang and Huang, Chaoying (1998): Some aspects of desertification deriving from sand and dust storms in North-western China. *First LAS/WMO International Symposium on Sand and Dust Storms (ISSDS-1), WMO/TD-No.864*, 313-318.

Wu, Zheng (1997): *Research on Inland Sand Deserts and Coastal Dunes in China*. Science Press, Beijing, China, 143p. (in Chinese)

Xia, Xuncheng and Yang, Gensheng (1996): *Damages by Sand and Dust Storms and Countermeasures for Them in Northwest China*. Chinese Science-Environment Publisher, Beijing, 128p. (in Chinese)

Xinjiang Uygur Zizhiqu, Regional Geography Editorial Committee and Xinjiang Regional Geography and Climatography Editorial Committee (1995): *Xinjiang Regional Geography, Volume 10, Climatography*. Xinjiang People's Press, Ürümqi, 413p. (in Chinese)

Xu, Quiyun and Ho, Jingsong (1997): Analysis on time and space distributions of sand and dust storm weather in the northwest region of China. *In* Fang, Zong-you *et al.* eds., *Studies on Sand and Dust Storms in China*, Meteorology Press, Beijing, 11-15. (in Chinese)

Yoshino, M. (1992): Wind and rain in the desert region of Xinjiang. Northwest China. *Erdkunde (Bonn)*, **46**: 203-216.

Yoshino, M. (1995): Climatic fluctuation, desertification and human activity in the oases in the Taklimakan desert (2) — Population change and meteorological disasters —. *Bungaku Ronso of Aichi University*, **110**: 1-23. (in Japanese with English abstract)

Yoshino, M. (1997): *Desertification in China*. Taimeido, Tokyo, 300p. (in Japanese)

Yoshino, M. (1998): An overview and problems of the climatological and human geographical studies on dust storm. *J. Arid Land Studies*, **8**: 165-168. (in Japanese with English abstract)

Yoshino, M., Fujita, Y., Arizono, S., Du, M. and Lei, J.-q. (1996): Impacts of agricultural land use on desertification in the Taklimakan Desert. *J. Arid Land Studies*, **5**: 107-115. (in Japanese with English abstract)

Zhang, De'er (1982): An analysis on "rain-dust" phenomena during the historical period. *Kexuetongbao*, 27: 294-297 (in Chinese).

Zhang, De'er (1984): A preliminary analysis on synoptic climatology of falling dust since the historical period in China. *Scientia Sinica*, 27B: 278-288; 825-836.

Zhao, Zongci (1996): Climate change and sustainable development in China's semi-arid regions. *In* Ribot, J.C., Magalhaes, A.R. and Panagides, S.S. eds.: *Climate Variability, Cimate Change and Social Vulnerability, in the Semi-arid Tropics*, Cambridge University Press, Cambridge, 92-108.

Zheng, Xinjiang and Chao, Yaming (1997): Distribution of sand and dust storms and cloud patterns in the northwest region. *In* Fang, Zong-you *et al.* eds., *Studies on Sand and Dust Storms in China*, Meteorology Press, Beijing, 92-97. (in Chinese)

Zhu, Fukang and Zhang, Wengian (1998): The dust storm in China. *First LAS/WMO International Symposium on Sand and Dust Storms, WMO/TD-No.864*, 1-6.

Zhu, Zhenda (1984): Aeolian landforms in the Taklimakan Desert. *In* El-Baz, F. ed., *Deserts and Arid Lands*, Martinus Nijhoff Publ., The Hague, 133-143.

沙漠研究 10-3, 183-188 (2000)
Journal of Arid Land Studies

— Original Article —

A Simple Model for Dust Emission

SHAO Yaping* and LU Hua*

1. Introduction

Dust emission rate, F, has been conventionally expressed as a function of friction velocity, u_*. The field measurements of Gillette (1981), Gillette and Walker (1977), Nickling and Gillies (1989), Nickling and Gillies (1993) show that dust emission rate is in general proportional to u_*^n with n varying between 2 and 5. There is a large scatter in the observed data. The wind tunnel experiments of shao *et al.* (1993) show that saltation bombardment is mainly responsible for dust emission and that the vertical dust flux is proportional to horizontal sand drift intensity. They also proposed a theory based on the concept of particle binding energy and the energy balance during the collision between saltating particles and the surface.

The model of Shao *et al.* (1993) has two major intrinsic problems. First, it is difficult to accurately estimate the dust particle binding energy on either theoretical or experimental grounds. It can be shown that the uncertainty involved in the theoretical estimation of dust particle binding energy is several orders of magnitude. Second, during particle and surface collision, the kinetic energy of saltating particles is not conservative, as a proportion of the particle kinetic energy is converted to heat.

In this short paper, we describe a new dust emission model that is still based on the assumption that saltation bombardment is mainly responsible for dust emission, but uses a different formulation in the calculation of dust emission.

2. Dust Emission Model

The proposed mechanism for dust emission by saltation bombardment is based on the observation that sand grains saltating over a surface of loose fine particles excavate ovoid shaped craters in the bed. This observation leads to the construction of the model that calculates the crater volume and dust release created by individual saltating particles. Dust emission due to a large number of saltating particles can then be estimated by a superposition of individual impacting events.

Several assumptions are made to derive the model, as listed below.

1. Impact particles have no initial rotation and small rotation during the ploughing process. If follows that for polyhedral particles, $X_T \simeq X + \frac{d}{2}\phi$ and $Y_T \simeq Y$, with ϕ being the rotation angle as shown in Fig. 1.
2. The ratio of the vertical force to the horizontal force on the particle during ploughing is a constant K.
3. A constant plastic flow pressure exists during ploughing and its horizontal component is denoted by p;
4. The depth over which surface contacts the particle is the same as that of the crater, Y_T, as illustrated in Fig. 1.
5. The removed volume is the product of the area swept out by the particle tip and the width b of ploughing face.

$$V = b\int Y_T dX_T = \int_0^{t_c} Y_T \frac{dX_T}{dt}\, dt$$

where t_c is the time at which ploughing ceases;

6. The vertical and horizontal forces on the particle are located at the centre of the surface soil material in contact with the particle. The symmetrical picture of two-dimensional ploughing shown in Fig. 1 can be understood as the average situation for grains which are tilted in either direction as they strike the surface. To be consistent with Assumption 2, the projected contact area in the horizontal plane is twice that in the

* School of Mathematics, University of New South Wales, Sydney Australia.

(Received, July 26, 1999; Accepted, September 10, 1999)

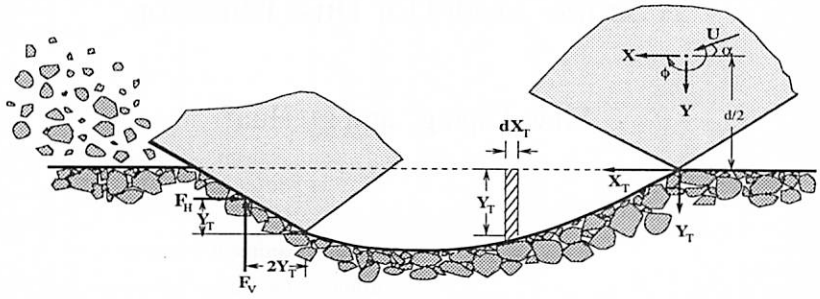

Fig. 1. A schematic illustration of the saltation bombardment process. A saltating particle ploughes through the soil, creates a small crater and ejects particles into the air. The horizontal nd vertical components of the force exerted on the particle by the target soil are $F_H = pYb$ and $F_V = KpYb$, respectively. See text for more details.

vertical plane.

The equations of particle motion in the X and Y directions and the equation of angular rotation are

$$m\frac{d^2X}{dt^2} + pYb = 0 \tag{1}$$

$$m\frac{d^2Y}{dt^2} + KpYb = 0 \tag{2}$$

$$I\frac{d^2\phi}{dt^2} + pbY\left(\frac{d}{2} - Y\right) - 2(KpYb)Y = 0 \tag{3}$$

where ${}_pY_b$ and K_pY_b are the horizontal and vertical components of the resistance force acting upon the ploughing particle. It is assumed the $Y_T = Y$ and $X_T = X + \frac{d}{2}\phi$.

Using the conditions that $Y|_{t=0} = 0$ and $\frac{dY}{dt}|_{t=0} = U\sin\alpha$, $\frac{dX}{dt}|_{t=0} = U\cos\alpha$ and $X|_{t=0} = 0$ the solutions of the above equation system are

$$X(t) = \frac{U\sin\alpha}{\beta K}\sin\beta t + \left(U\cos\alpha - \frac{U\sin\alpha}{K}\right)t \tag{4}$$

$$Y(t) = \frac{U}{\beta}\sin\alpha\ \sin\beta t \tag{5}$$

$$\phi(t) = \frac{3.75U^2\sin^2\alpha}{\beta^2 d^2}[2(\beta t)^2 + \cos 2\beta t - 1] + \frac{3U\sin\alpha}{\beta d}(\sin\beta t - \beta t) \tag{6}$$

and where $\beta = \sqrt{\frac{pKb}{m}}$.

1) Volume Removal

It follows from assumption 5 and Eq. (4), (5) and (6), the volume removed by a single impact can be calculated. there are two cases. In Case 1, the impact particle ploughes into the target soil and subsequently leaves it when Y_T becomes zero. In Case 2, the particle stops during its scooping action at some depth as its kinetic energy is exhausted. For Case 1, the volume removal can be calculated using

$$\frac{V}{b} = \frac{U^2}{\beta^2}(\sin 2\alpha - 4\sin^2\alpha) + \frac{7.5\pi U^3\sin^3\alpha}{\beta^3 d} \tag{7}$$

Case 2 has been discussed by Lu and Shao (1999).

2) Vertical Dust Flux

We first consider the dust emission by saltation bombardment from a soil that contains multisized dust particles and uniform sand particles (with diameter d). If n_s is the particle number flux density (number of impacting particles per unit area per unit time) and f is the fraction of dust contained in V, the vertical dust flux caused by saltation bombardment can be calculated by

$$F(d) = c_N n_s \rho_b f \mathrm{V} \tag{8}$$

where ρ_b is the bulk density of soil and c_N is a constant of proportionality less than 1, as a proportion of dust particles may stick on aggregates ocntained in V. Following the well developed line of sand saltation momentum transfer near the surface, we have

$$n_s = \frac{\rho u_*^2(1 - u_{*t}^2/u_*^2)}{m(U_1\cos\alpha_1 - U\cos\alpha)} \tag{9}$$

where u_{*t} is the threshold friction velocity for sand particles, U_1, is the ejection velocity of sand particles and

Table 1. Soil parameters used for calculation of sand drift Q for comparison with the experimental data of Gillette (1977).

	S1	S2	S3	S4	S5	S6	S9
Soil moisture (%)	0.8	0.99	1.0	0.5	0.65	0.75	6.6
Non-erodible elements	0.6	0.1	0.05	1.5	1	0.05	0.01
Observed u_{*t} (m/s)	0.25	0.25	0.25	0.25	0.25	0.52-0.6	0.65
Simulated u_{*t}	0.2561	0.2576	0.2572	0.2542	0.2545	0.2430	0.9142

α_1 the ejection angle.

Substituting (9) and (7) into (8), we obtain

$$F(d)=\frac{c_N f\rho_b U^2}{2p}\left(\sin 2\alpha-4\sin^2\alpha+\frac{7.5\pi U\sin^3\alpha}{\beta d}\right)\times\frac{\rho u_*^2(1-u_{*t}^2/u_*^2)}{U_1\cos\alpha_1-U\cos\alpha} \quad (10)$$

Following Owen (1964), the horizontal saltation flux for a dry soil with uniform particles is

$$Q(d)=\frac{c\rho u_*^3}{g}(1-u_{*t}^2/u_*^2) \quad (11)$$

where c is Owen's coefficient and g is gravitational acceleration. (10) can be expressed in term of Q(d) as

$$F(d)=\frac{C_\alpha g f\rho_b}{2p}\left(\sin 2\alpha-4\sin^2\alpha+C_\beta u_*\sqrt{\frac{\rho_p}{p}}\right)Q(d) \quad (12)$$

where C_α is a coefficient of order $10c_N$ and C_β is a coefficient of order 1. Eq. (12), then, can be simplified as

$$F(d)=\frac{C_\alpha g f\rho_b}{2p}\left(0.24+C_\beta u_*\sqrt{\frac{\rho_p}{p}}\right)Q(d) \quad (13)$$

To estimate dust emission rate from soils with a particle size distribution $p(d)$, we separate soil particles into the categories of dust and sand. An integration of Eq. (13) over sand particle sizes gives the total dust emission rate F induced by saltation bombardment of sand grains of all sizes

$$F=\int_{d_1}^{d_2}F(d)p(d)\,\delta d \quad (14)$$

where d_1 and d_2 are the low and upper bound of sand particle diameters. The ratio between the total vertical dust flux and total horizontal sand flux is

$$\frac{F}{Q}=\frac{\int_{d_1}^{d_2}F(d)p(d)\,\delta d}{\int_{d_1}^{d_2}Q(d)p(d)\,\delta d} \quad (15)$$

As an approximation, it is possible to simplify the above equation as

$$\frac{F}{Q}=\frac{C_\alpha g f\rho_b}{2p}\left(0.24+C_\beta u^*\sqrt{\frac{\rho_p}{p}}\right) \quad (16)$$

which is a simple rearrangement of (13).

Eq. (16) tells us several qualitatively important relationships: (a) since Q is proportional to u_*^3, F must be proportional to u_*^i with $i=3\sim4$; (b) the saltation bombardment efficiency ratio, F/Q, is linearly proportional to the fraction of dusts contained in the parent soil, f, and inversely proportional to soil surface hardness parameter, p^{k_1}, with $k_1=1\sim1.5$. For large p (hard surface), $k_1\simeq1$ and for smaller p (soft surface), $k_1\simeq1.5$; (c) for sufficiently large p so that $C_\beta u_*\sqrt{\frac{\rho_p}{p}}\ll0.24$, F/Q would be independent of u_*, while for sufficiently small p so that $C_\beta u_*\sqrt{\frac{\rho_p}{p}}\gg0.24$, F/Q increases linearly with u_*.

3. Comparison with Experiments

We now examine the performance of the dust emission model against the field measurements of Gillette (1977), using Eq. (14) and (13). According to Gillette, soils 1, 2, 4 and 5 have a sand, soil 3 a loamy sand, soil 6 a sandy loam and soil 9 a clay texture.

Two kinds of comparison are attempted for F. One is fully simulated and the other one is semi-simulated. The fully simulated F is done by first calculating Q using the saltation model of Shao *et al.* (1996), and then relating F to the predicted Q by Eq. (14). In order to use Eq. (16) to predict F, the value of p needs to be determined. The fitted values of F are called semi-simulated F.

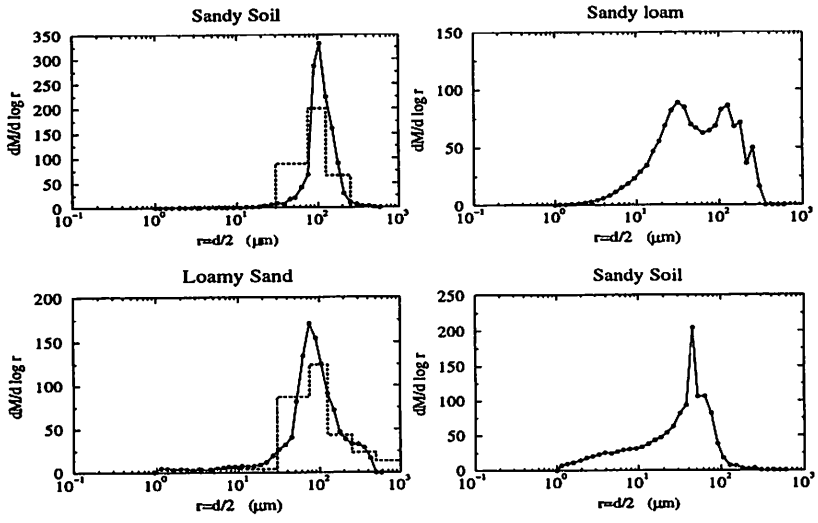

Fig. 2. Particle size distributions (PSD) for sand (soils 1, 2, 4 and 5), loamy sand (soil 3) comparison with the ones given in Gillette and Walker (1977). The dotted curve is the particle size distribution of Gillette and Walker and the soil curve is Australia soil PSD assigned. Assumed PSDs for sandy loam and clay used in the simulation are also shown.

One of the most important parameters for simulating Q is the threshold friction velocity. u_{*t}. The calculation of the threshold velocity, u_{*t}, for saltating particles follows Shao *et al.* (1996). The measured values of u_{*t} for each soil type are explicitly given by Gillette (1977, 1988).

To calculate Q, dry sieving soil particle distributions of Soil 3 and Soil 4 (given by Gillette and Walker (1977)) are used in our simulation (Fig. 2). The particle size distribution of soils 1, 2 and 5 is assumed to be the same as Soil 4. To test the effect of particle size distribution, we replace the particle size distribution of Soil 4 by an Australia sandy soil and also used it for the simulation of soil 1, 2 and 5. Similarly, the PSD of soil 3 is replaced by an Australia loamy sand. The PSDs are shown in Fig. 2 compared with the ones of Gillette and Walker (1977). The MDPSDs for soil 6 and soil 9 are also selected among Australia typical loam and clay samples. They contain a similar amount of clay and silt particles as described by Gillette (1977) and have similar soil textures.

For all cases, we used $C_\beta = 1.37$, Owen's coefficient $c = 0.8$ and soil particle density $\rho_p = 2650$ kg/m^3. The values of f used are the fraction for $d < 50\mu$m given by Gillette (1977). We used $C_a = 5$ and $\rho_b = 1000$ kg/m^3.

Fig. 3 shows the comparison of simulated and observed horizontal sand fluxes, Q, and that of fully simulated (using simulated Q to calculate F), semi-simulated (using observed Q to calculate F) and observed vertical dust flux F, where Q and F and plotted against friction velocity, u_*, for soils 1 to 5. Although some parameters used for the simulation are roughly estimated, the predicted Q and F and observed Q and F and in good agreement for all soils, except soil 2. For soil 2, the simulated Q is about 5 times larger than observed while semi-simulated dust flux is smaller than both measured and fully simulated. This indicates that soil 2 may have a different particle size distribution (the typical mode may be not close to 180μm) although is classified as a sandy soil. Overall, given the uncertainties involved in both the measurements and the modeling, the agreement in Fig. 3 provides encouragement that the model has produced satisfactory estimates of streamwise sand fluxes and vertical dust fluxes.

4. Conclusions

In this short paper, we have presented a new dust emission model based on the understanding that dust emission is mainly caused by saltation bombardment. The prediction of dust emission rate is achieved through

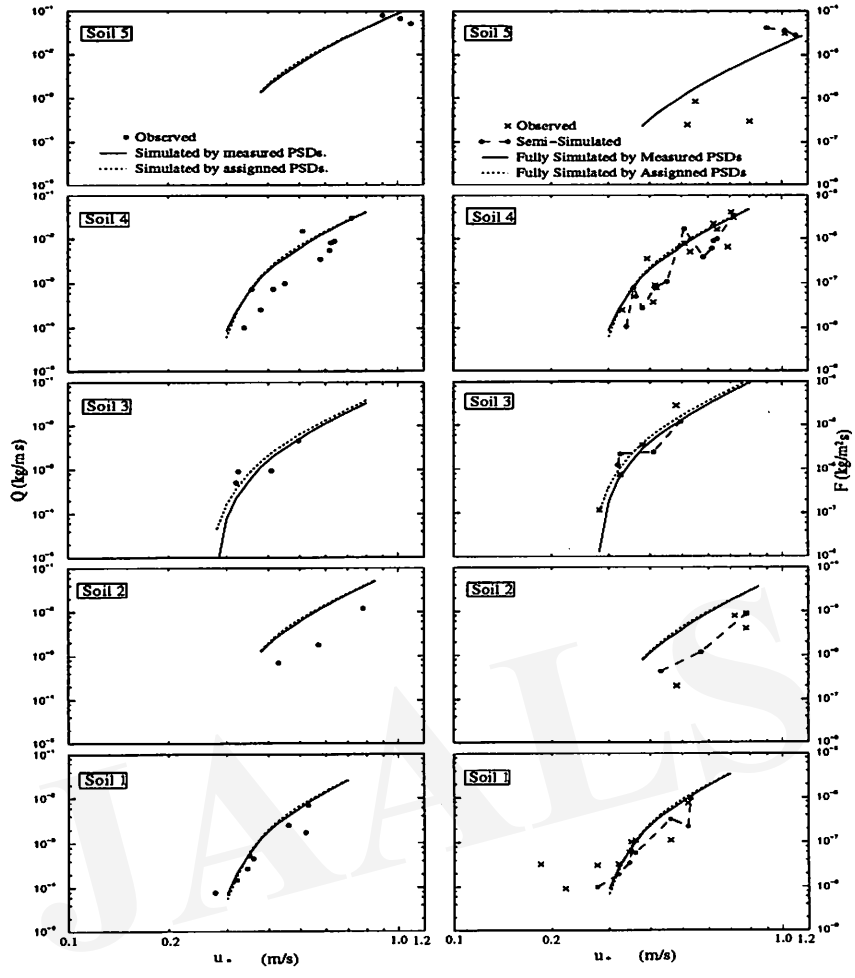

Fig. 3. Comparison of simulated using PSDs of Gillette and Walker (1977) (solid curve), simulated using assigned PSDs, and observed (full circles) horizontal sand drift Q (left side) and that of fully simulated (solid curve: using predicted Q by PSDs of Gillette and Walker (1977); dotted curve: using predicted Q by assigned PSDs), semi-simulated (using observed Q, dashed curve plus open circle) and observed (full circles) vertical dust flux F versus friction velocity, u_*, for Gillette (1977) soils 1 to 5.

modeling the ploughing process of individual saltating sand grains and the resulted volume removal of the surface soil. It has been found that the crater volume removal is proportional to the impacting particle velocity, $V \propto U^n$, the vertical dust emission rate is proportional to friction velocity, $F \propto u_*^{n+1}$, with n being around 2 to 3. For practical purposes, the vertical dust flux can be calculated using Eq. (15) or Eq. (16) for simplicity.

References

Gillette, D.A. (1977): Fine particulate emission due to wind erosion. *Transactions of the ASAE*, 20: 890-897.

Gillette, D.A. (1981): Produciton of dust that may be carried great distances. *Spec. Pap. Geol. Soc. Amer.*, 186: 11-26.

Gillette, D.A. (1998): Threshold Friciton velocities for dust production for agricultural soils. *J. Geophys. Res.*, 93: 12645-12662.

Gillette, D.A. and Walker, T.R. (1977): Characteristics of airborne particles produced by wind erosion on sandy soil, high plains of west Texas. *Soil Science*, 123: 97-110.

Lu, H. and Shao, Y. (1999): A new model for dust emission by saltation bombardment. *J. Geophys. Res.*, 104 (D14): 16827-16842.

Nickling, W.G. and Gillies, J.A. (1989): Emission of fine-graned particulates from desert soils. *In* Leinen, M. and Sarnthein, M.

eds., *Paleoclimatology and Paleometeorology: Modern and Past Patterns of Global Atmospheric Transport*, Kluwer, 133-165.

Nickling, W.G. and Gillies, J.A. (1993): Dust emission and transport in Mali, West Africa. *Sedimentology*, 40: 859-868.

Owen, R.P. (1964): Saltation of uniform grains in air. *J. Fluid Mech.*, 20: 225-242.

Shao, Y., Raupach, M.R. and Findlater, P.A. (1993): The effect of saltation bombardment on the entrainment of dust by wind. *J. Geophys. Res.*, 98: 12719-12726.

Shao, Y., Raupach, M.R. and Leys, J.F. (1996): A model for predicting aeolian sand drift and dust entrainment on scales from paddock to region. *Aust. J. Soil Res.*, 34: 309-342.

沙漠研究 10-3, 189-197 (2000)
Journal of Arid Land Studies

— Original Article —

Aeolian Transport of Particles in Chernobyl and Application to Dune Morphology

HATANO Yuko* and HATANO Naomichi**

We review our recent proposal for modeling long-term radioactive dust migration in Chernobyl. We emphasize the importance of fractal wind fluctuation, namely the Corrsin-Obukhov relation of turbulent flow. Theoretical predictions derived from the model are in remarkable agreement with data of the radionuclide concentration measured near Chernobyl over a decade. One of the predictions shows that the concentration of radioactive aerosol decreases in time as, where and are fitting parameters. The fractal exponent -4/3 is essential in fitting the long-term measurement data.

We also apply the same principle to an aeolian dune problem; we carried out numerical simulation based on Werner's model, incorporating the Corrsin-Obukhov relation of the wind velocity. It is shown that the fractal wind fluctuation yields dome dunes, which have never been reproduced by numerical calculations before.

Key Words: Barchans, Linear dune, Dust Chernobyl

1. Introduction

This paper concerns transport phenomena by wind, both (i) migration of radioactive aerosols in Chernobyl and (ii) sand transport in deserts. We first review our study on transport of radioactive particles in Chernobyl in the former part of the paper. In the latter part, we apply the findings in the study to dune morphology.

The Chernobyl nuclear power plant accident in 1986 spread a large amount of radionuclides into the environment. Many simulational studies have been done as to how the pollutants from the accident migrate. However, the primary subject of such studies was emergency evacuation planning, and hence their target period was at most several weeks after the accident. After the target period, the simulation results do not agree with measured data. Now it is the major issue to predict long-term behavior of the pollutants that are resuspended from the soil surface as aerosols.

For this purpose, we recently introduced a novel model of long-term aerosol migration (Hatano and Hatano, 1997; Hatano *et al.*, 1998a). We discovered that, in order to reproduce actual measurement data in Chernobyl over ten years, it is crucial to take account of long-term temporal correlation of the wind velocity. According to the Corrsin-Obukhov relation in the field of turbulence theory (Monin and Yaglom, 1975), the temporal correlation of the wind velocity follows the power law

$$\langle V_i(t)\, V_i(t+\tau)\rangle \sim \tau^{-2/3} \qquad (1)$$

for large τ, where $V_i(t)$ is the wind velocity in the ith direction (i=1,2) at time t. This fractal power law is essential in reproducing the Chernobyl data.

In the present paper, we first review theoretical predictions of our aerosol-migration model and compare them with actual data measured in Chernobyl. Since the Corrsin-Obukhov relation is a universal law over wide

* Institute of Physical and Chemical Research (RIKEN). Wako, Saitama 351-0198, Japan.
** Department of Physics, Aoyama Gakuin University. Chitosedai, Setagaya, Tokyo 157-8572, Japan.

(Received, March 10, 1999; Accepted, January 11, 2000)

range of time scale and length scale, we expect that the fractal correlation should reveal itself in various phenomena of aeolian dynamics besides the Chernobyl case. From this point of view, we also report new results of numerical simulation of dune morphology; we show that the time correlation of the wind velocity is an essential element of formation of dome dunes.

To emphasize novel features of our aerosol-migration model, let us first present several theoretical predictions of the model for the Chernobyl case:

(i) The aerosol concentration C of each radionuclide at a fixed location decreases after its emission as

$$C(t) \simeq Ae^{-\Lambda t} t^{-4/3} \tag{2}$$

for large t, where t is the days since the accident, A is a constant that is proportional to the quantity of the initial deposition, and Λ is an effective removal rate, that is, the sum of reaction constants of all first-order kinetics that remove the nuclide from the resuspension-deposition cycle; *i.e.* λ=(radioactive decay const.)+(water runoff rate)+(vegetation uptake rate)+...

(ii) The resuspension factor K (the ratio of the radionuclide concentration in the air to that on the soil surface) decreases in time as

$$K(t) \sim t^{-4/3} \tag{3}$$

for large t. The resuspension rate is an important quantity from a practical point of view, because it is directly related to lung cancer risk. However, the time dependence had been rarely understood.

(iii) The standard deviation $\sigma(T)$ of the concentration data during T days depends on T as

$$\sigma(T) \sim T^{-1/3} \tag{4}$$

Here T is the averaging period of the time series; the concentration is divided into N bins of length T, then averaged within each bin throughout the data. If we increase T, the standard deviation should decrease. We stress that the dependence of σ on T of the present model is of a fractal type and completely different from white-noise fluctuation. For further details of calculation of σ and the significance of Eq. (4), refer to Hatano and Hatano (1997). In short, the exponent -1/3 smaller than 0 but larger than -1/2 indicates fractal fluctuation of the data.

(iv) Our theoretical model indicates that the spatial distribution of the radionuclide is a Gaussian distribution whose half-width increases in time as $t^{2/3}$. This increase is faster than the normal-diffusion case $t^{1/2}$.

The first three predictions are in remarkable agreement with data of the aerosol concentration measured near Chernobyl over a decade. The fourth prediction is yet to be confirmed because of lack of data.

We provide in Section 2 more details on the accident and the measurement data that we used. In Section 3, we describe our modeling of aerosol migration. The first three predictions of the model are compared with measured data in Section 4. We turn our attention to a different problem in section 5, namely dune morphology. We report results of numerical simulation that incorporates the Corrsin-Obukhov relation and show an interesting effect of the time correlation on dune formation. Section 6 provides a summary and discussions.

2. Chernobyl Accident and Garger Measurement

The Chernobyl accident occurred on April 26, 1986. The reactor is located at about 16 km northwest to the town of Chernobyl in Ukraine, near the border with Belarus. Figure 1 shows details of the accident: the smoke due to the fire of the fourth unit of the power plant first rose in the troposphere. Although a small portion of the released radionuclides reached the stratosphere and contaminated the northern hemisphere as fallout, most were contained in the plume in the troposphere and carried all over Europe. Heavy particles dropped near the power plant, while lighter ones traveled up to hundreds of kilometers. The deposits from the plume during the first few weeks are referred to as acute deposits. These acute deposits have migrated as aerosols through aeolian resuspension and have contaminated the air of the region for years after the accident. Although the plume disappeared soon after the fire was extinguished, the air contamination still persists due to the resuspension-deposition process.

The most contaminated area is within 30 km of the power plant (Garger, 1994). It is estimated that about 6 tons of nuclear fuel (2×10^{18} Bq of radioactive nuclides) were deposited in this area. The nuclides of significant quantity were ^{137}Cs, ^{134}Cs, ^{144}Ce, ^{106}Ru, and ^{90}Sr. The soil

in the area is moist and consists mostly of *podzol* (94%). The topography is almost flat. The land use is primarily grass and crop land. Forests are the second largest land cover (30-35%). Only a small part of the area is residential.

Since the accident, the radioactivity in the air has been measured on a daily basis at several points within 30 km (Garger, 1994). For the locations of the measurement sites, see the map in Hatano *et al.* (1998a). The measurement is done with a high-volume sampler with a flow rate of $10^5 m^3$/day. The height of the sampler is 1.5 m above the ground. A filter in the sampler traps particles less than 15μm in diameter. The area of the filter is $1.05 m^2$.

3. Model with Fractal Wind Fluctuation

We here review our model of aerosol migration (Hatano and Hatano, 1997; Hatano *et al.*, 1998a). Although the model might appear to be simple, it should be stressed that its predictions are in a good agreement with the measured data at Chernobyl. The present model captures an essential feature of long-term behavior of aerosol migration caused by aeolian resuspension from the soil surface.

In the resuspension-deposition cycle a dust particle is suspended by wind (resuspension), blown for a certain time (advection, or transport), and deposited because of the gravitational setting (See Fig. 1). While the particle stays in the air, its transport depends on the wind velocity and direction at that time. The wind velocity and direction change from time to time, and hence the transport varies as well. It may be intuitive to point out a theoretical similarity between our model and the Brownian motion. The Brownian motion is caused by an external force that hits the particle from a random direction and in random magnitude. The random external force corresponds to the wind in our model.

On the basis of the above consideration, we introduced a two-dimensional advection equation that describes the aerosol migration of dust particles (Hatano and Hatano, 1997; Hatano et *al.*, 1998a):

$$\frac{\partial C}{\partial t} + v_x \frac{\partial C}{\partial x} + v_y \frac{\partial C}{\partial y} + \Lambda C = \delta(t)\,\delta(x)\,\delta(y). \quad (5)$$

The term ΛC represents processes in which a certain proportion of the amount of the radionuclide is removed constantly from the cycle. Besides radioactive decay, various effects such as sorption to the soil and vegetation uptake have been studied in the form of this term under the name of the "linear compartment model" see *e.g.* Chamberlain (1970). The product of the delta functions in the right-hand side of Eq. (5) is the source term that corresponds to the acute deposit of the power-plant accident.

The variables $\vec{v} = (v_x, v_y)$ are the mean transport velocity of the aerosol. The aerosol particles move along the path of the wind when they are resuspended from the ground. Thus the transport velocity v_i $(i = x, y)$ should be approximately proportional to the actual wind velocity V_i in the form

$$v_i \simeq \frac{\bar{\tau}_1}{\bar{\tau}_0 + \bar{\tau}_1} V_i, \quad (6)$$

where $\bar{\tau}_0$ is the average time for which a dust particle remains in the state of deposition, and $\bar{\tau}_1$ is the average time in the state of suspension-advection. Thus we require of the variables v_x and v_y to be random and to follow the Corrsin-Obukhov relation (1):

$$\langle v_i(t')\, v_i(t) \rangle \sim \begin{cases} |t'-t|^{-2/3} & \text{for } i=j, \\ 0 & \text{for } i \neq j, \end{cases} \quad (7)$$

Here the brackets denote the average with respect to

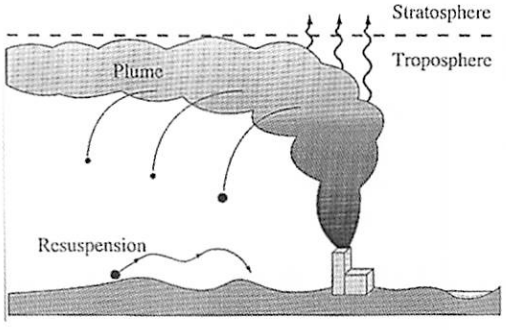

Fig. 1. A schematic of the Chernobyl accident. Radionuclides were carried in the plume due to the fire, deposited to the ground surface, and attached to dust particles and migrate. A typical migration process of radioactive dust is shown in the lower left part of the figure. Each particle is convected by the wind and deposited because of the gravity. Since wind blows randomly (but with correlation), the projection of the particle movement onto the horizontal plane resembles the Brownian motion. Nuclides in the resuspension-deposition cycle decrease by various processes: for example, radioactive decay, permeation into the soil as water solution, uptake by plants, and immobilizing chemical reactions with soil.

the randomness of the wind velocity.

The governing equation (5) is thus a stochastic differential equation. There is a solution for each specification of the time dependence of the stochastic variables $\vec{v}(t)$. The final goal is to obtain quantities averaged over all possible forms of the function $\vec{v}(t)$. Although the equation (5) does not have any diffusion terms explicitly, the randomness of $\vec{v}(t)$ results in "macroscopic diffusion" (Kapoor and Gelhar, 1994) in the same way that the random force results in diffusion of the Brownian particle. For details of the solution of such a diffusion equation, see Hatano *et al.* (1995).

4. Comparison of Theoretical Predictions with Actual Data

In the following, we compare our theoretical predictions (i)-(iii) in Section 1 with available data of aerosol migration in Chernobyl.

1) Concentration decrease

The solution of the "macroscopic diffusion" equation yields the average concentration in the form $\langle C(t) \rangle \sim e^{-\Lambda t^{-4/3}}$, which is our first prediction Eq. (2). This prediction explains the Chernobyl data very well with only two parameters A and Λ adjusted.

To exemplify the agreement between the prediction and the data, we plotted in Fig. 2 the six-month average for data of ^{134}Cs and ^{137}Cs measured at four kilometers east of the plant. Let us remark that cesium has been used as a well-behaving tracer in aeolian dynamics studies; see *e.g.* Chappell (1996). The solid curves in the same figures are fitting curves based on Eq. (2). The curves are remarkably consistent with the measurement data within statistical accuracy.

Note that the power-law factor in Eq. (2) is essential in explaining the time dependence, particularly for the first 1000 days. The measurement data are not fit when only the exponential factor is used; an exponential factor typically appears in the widely used linear compartment model (*e.g.*, Chamberlain, 1970). Because of the power-law factor, the predicted concentration becomes significantly smaller in a long period than the predictions of the linear compartment model. The difference is up to a few orders of magnitude.

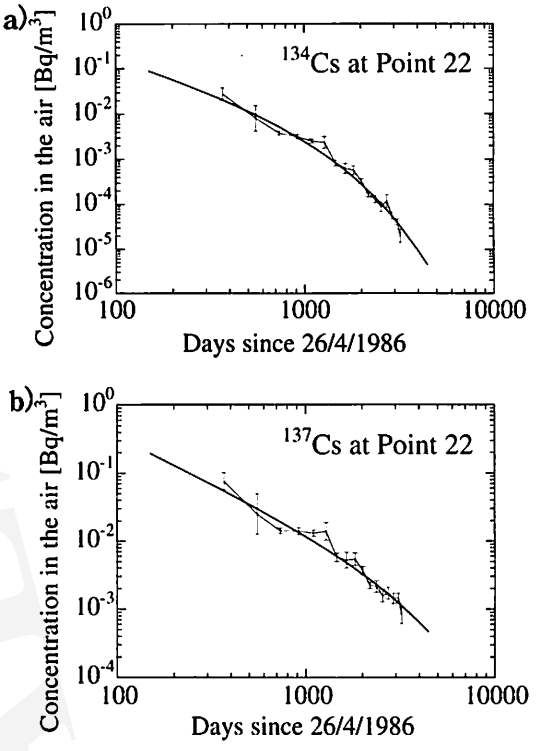

Fig. 2. Six-month averages of the concentration of ^{134}Cs and ^{137}Cs at Point 22, and the best-fit curves with Eq. (2) (solid line).

2) Resuspension factor

Our model also yields a prediction of the resuspension factor. Let us first summarize facts about the resuspension factor. The resuspension factor, the ratio between the airborne concentration and the surface concentration is 10^{-6} (Nicholson, 1988). The soil specific radioactivity is much larger than the airborne specific radioactivity in general (Hollsänder and Garger, 1996), and that most of the radionuclides in the soil (particularly ^{137}Cs) exist as immobile (*i.e.*, unable to be resuspended)chemicals (Watanabe *et al.*, 1996). Hence the denominator of the resuspension factor (the nuclide concentration on the ground surface) is dominated by the amount of nuclides *remaining in place* on the ground, and is scarcely affected by the amount resuspended from the ground. The concentration staying in place on the ground decays only exponentially, while the decay of the aerosol concentration has the power-law factor due to the diffusion, as

shown in Eq. (2). Thus we have

$$K(t) \sim \frac{e^{-\Lambda t} t^{-4/3}}{e^{-\Lambda t}} = t^{-4/3}. \quad (8)$$

This is our theoretical formula for the resuspension factor.

For the actual Chernobyl data, Garger *et al.* (1997) found empirically that a power-law function fits the resuspension data very well. They estimated the exponent by fitting the function to the data as follows;

$$K(t) \sim t^{-1.4}. \quad (9)$$

This exponent estimate is close to our theoretical prediction -4/3. As is shown in Fig. 3, the existing theories fail to explain the measurement data. In contrast, our theoretical prediction is in good agreement with Garger *et al.*'s best fit.

The measured data in Fig. 3 shows the seasonal cycle; in winter, the resuspension factor becomes smaller than in summer, because snow covers the soil surface. However, we are interested in behavior in a longer time scale. As shown in Fig. 3, Garger's fit (and hence our prediction) explains the data well if we average out the seasonal variation.

3) Concentration fluctuation

Another theoretical prediction is the power law Eq. (4). The exponent in Eq. (4), namely -1/3, agrees remarkably with Garger *et al.*'s experimental result -0.33 ± 0.08 (1994). They calculated $\sigma(T)$ for $T = 2, 3, 4, 6, 10, 15, 20,$ 30, and 60 days during the years 1987-1991. The exponent estimate 0.33 ± 0.08 was obtained as the average of estimates for the five years and two sites near Chernobyl.

Furthermore, a similar result was obtained in Gifford's study (1991) on a completely independent incident. He showed that the exponent of $\sigma(T)$ is -0.35 for atmospheric eddy sizes of several hundred kilometers, using data of the concentration of ^{85}Kr from a US nuclear facility over nineteen months and one thousand kilometers. Yet in another study on aerosol transport in the Arctic (Hatano *et al.*, 1998b), we found the exponents -0.36 ± 0.06 for cloud-condensation particles and -0.27 ± 0.08 for radon.

These studies imply that the relation $\sigma(T) \sim T^{-1/3}$ may

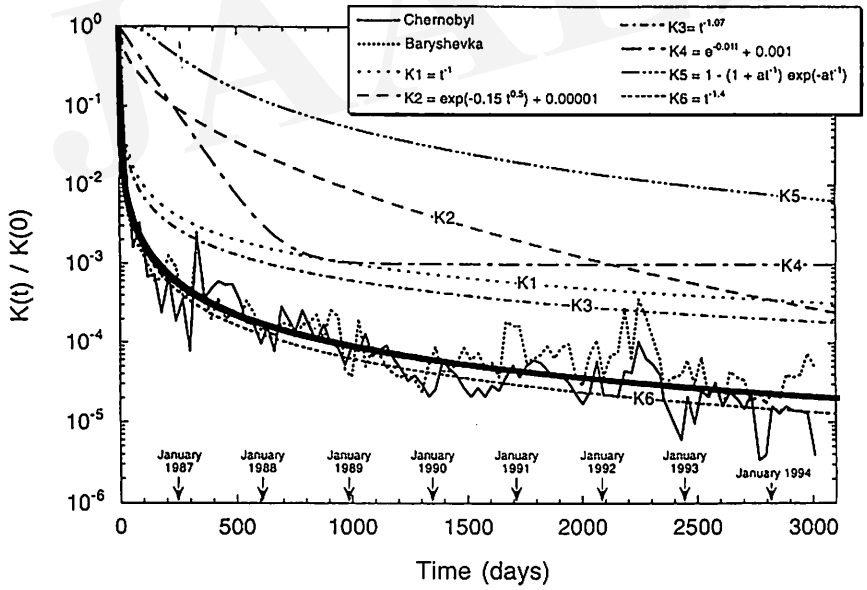

Fig. 3. The fitting of the measured resuspension factor (Garger *et al.*, 1997) to data from two measurement sites: the town of Chernobyl (16 km south to the power plant) and Baryshevka (160 km south to the plant). The data were normalized by the initial resuspension factor K (0). The fitting curves are the following. The thickest line is our prediction $t^{-4/3}$ or Eq. (8). (K1) the Garland model (1991); (K2) the Anspaugh model (1975); (K3) the Hoetzl model (1992); (K4) the Linsley model (1978); (K5) the Makhonko model (1992); (K6) Garger's empirical fit, *i.e.* Equation (9) in thepresent paper. All the previous models (K1-K5) fail to fit the measurement data. Garger *et al.* (1997) tried various functions and found that Eq. (9), or K6, fits the data well. Our prediction also fits the data well.

be a common law for large-scale aerosol transport. We claim that the Corrsin-Obukhov relation is behind this law. In other words, it is necessary to incorporate the fractal correlation when one studies long-term large-scale atmospheric dynamics of wind transport of aerosols.

We stress here that various microscopic aspects of aerosol migration are *phenomenologically* incorporated into the present model. This feature of the model greatly enhances its applicability to various situations of aerosol migration. Different places have different characteristics of soil surface, vegetation uptake, etc. These differences can be taken into account by changing the model parameter Λ and the prefactor of Eq. (2). Thus our predictions may be realized not only in Chernobyl but in different situations with different time and length scales.

5. Wind Correlation in Dune Morphology

We have seen that the fractal correlation of the wind velocity, Eq. (1), is essential in description of aerosol migration in Chernobyl as well as the ^{85}Kr data and the Arctic data. We naturally expect that the same principle should apply to description of other phenomena of aeolian dynamics.

Here we present our new results on sand dune dynamics. Saltation of sand particles phenomenologically resembles resuspension of aerosol except for the time scale of the dynamics. Hence we expect that transport of sand particles is essentially similar to the dynamics described by the stochastic differential equation Eq. (5). As we emphasized at the end of Section 4, the difference in time scale may be reduced to difference in the model parameter and the prefactor of Eq. (7).

Since it is rather hard to treat the equation analytically in the situation of sand dunes, we resort to numerical simulation. Indeed, Werner (1995) numerically simulated the aeolian dynamics of desert dunes in terms of the Brownian motion of sand particles. We can argue in the case of very small number of sand particles that the differential equation Eq. (5) corresponds to Werner's simulation with $\Lambda = 0$ (because the number of sand particles is conserved) and under an initial condition different from the delta function. (For a large number of particles, particle-particle interactions should come into the equation as non-linear terms such as C^2.)

An important point missing in his simulation is the fractal correlation of the wind velocity, Eq. (1); he used white noise for the sand-particle transport. In this section, we present a result of the simulation with correlated noise and thereby demonstrate that the correlation is essential in producing a type of sand dune, namely the dome type. The dome type of dune has never been produced by numerical simulation before.

Let us first explain Werner's model (Werner, 1995). Instead of treating huge number of sand particles, he introduced a coarse-grained viewpoint; in his model, sand "slabs" are transported on a two-dimensional lattice and form dunes. Each step of the simulation proceeds as follows. A sand slab is chosen randomly from those on the surface outside the shade of dunes. The slab is moved over a specified distance l in the direction of the wind. In most cases, the wind direction is chosen as a random vector $\vec{v} = (v_x, v_y)$. (In some cases, the wind direction was fixed throughout a simulation.) The slab may be deposited at the new site with a specific probability, otherwise moved further. The probability depends on whether the site has already slabs or not; it is lower if the site is the substrate, which is a place without other slabs. The move over the distance l is repeated until deposition. Then slabs may tumble down dunes until the entire pattern satisfies a condition of the angle of repose. This completes one simulation step. Then another slab is chosen to repeat the above process. Time t in the simulations is defined as the number of the steps divided by the number of the lattice sites.

We carried out the simulation, comparing the case where the random vector of the wind direction is white noise and the case with correlated noise. In the latter, the correlated noise was made to obey the Corrsin-Obukhov relation. To generate such a random sequence, we used a method by Makse *et al.* (1995). The initial distribution of slabs is random with the average height $H = 3$ in the present study.

In Fig. 4 we compare the results between the original Werner's model (uncorrelated case) and our model (correlated case). With temporal correlation of wind, the dune evolution is altered at least in one aspect: we observe clear barchan dunes in Fig. 4 (a-2) (correlated case), but not in Fig. 4 (a-1) (uncorrelated case). These barchan dunes change their direction from time to time ($t = 500$,

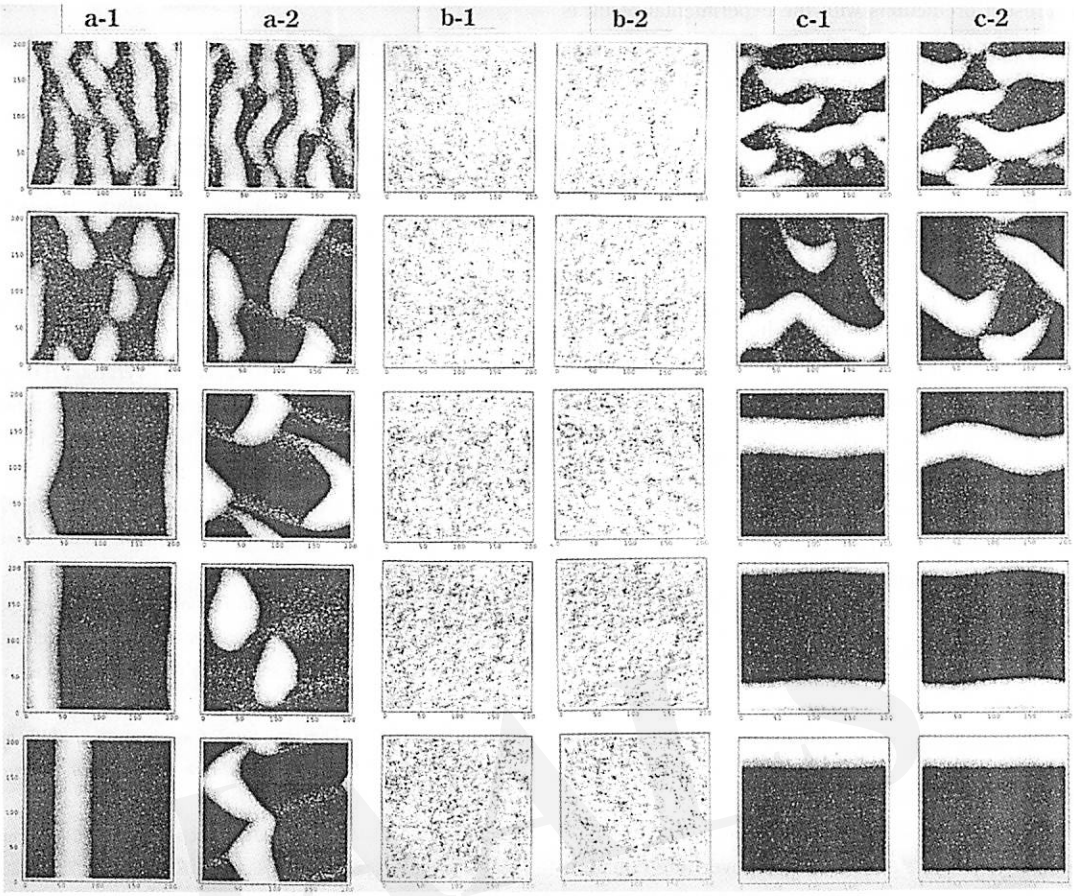

Fig. 4. Comparison between cases of uncorrelated/correlated winds.
Periodic boundary conditions were applied in all cases. Snapshots at t=100, 200, 500, 800, and 1500 from top to bottom. (a-1) Uncorrelated case. The wind velocity (v_x, v_y) was chosen from either (6, 2) or (-6, 2) randomly. Sand mounds are merged together to make a linear dune. (a-2) Correlated case. The wind velocity was chosen from ($\pm$6, 2) with correlation. Barchans are observed to change their direction, and dome-like dunes appear in between. (b-1) Uncorrelated case with (v_x, v_y)=($\pm$3, 3). (b-2) Correlated case with (v_x, v_y)=($\pm$3, 3). (c-1, 2) Uncorrelated and correlated cases with (v_x, v_y)=($\pm$2, 6).

1500 in Fig. 4 (a-1)). On intervals of dunes' direction changes, we observe dome-like dunes (t=800 in Fig. 4 (a-2)). In Figs. 4 (b), (c) the correlation scarcely affect the dune development.

The above result can be interpreted as follows. If wind blows in a correlated manner, the duration of the wind blowing from the same side should be larger, on average, than that in the uncorrelated case. While the wind blows sequentially from the same direc-tion (due to the correlation), barchan dunes are formed. When the wind direction inverses and the direction for a moment, the horn-like part of the barchans is blown off and the crest is eroded, and dome-like dunes will form. This is the first time where the dome dunes are reproduced.

6. Summary

To summarize, we emphasize the importance of temporal correlation of the wind in various phenomena of aeolian dynamics. In the preceding sections, we showed that our aerosol-migration model agrees excellently with the three quantities measured in Chernobyl ; the concentration, the fluctuation, and the resuspension factor. The predictions are based on a fundamental assumption of fractal correlation of the wind velocity, namely the Corrsin-Obukhov relation of turbulent theory. The agreement of

the present predictions with the experimental result is evidence for the validity of the assumption. In the dune-morphology simulation, we were able to reproduce dome dunes only after we introduced the time correlation of the wind.

This study is partly supproted by Sumitomo Funds.

Appendix

In this Appendix, we explain how we obtained the power-law Eq. (2), $C(t) \simeq Ae^{-\Lambda t} t^{-4/3}$. This formula is derived from an ordinary advection equation. Local wind blows radioactive aerosols in a specific direciton for a specific time. We include the effect of temporal correlation into the equation. The solution yields Eq. (2).

We introduced a two-dimensional advection equation that describes the aerosol migration of dust particles:

$$\frac{\partial C}{\partial t} + v_x \frac{\partial C}{\partial x} + v_y \frac{\partial C}{\partial y} + \Lambda C = \delta(t)\,\delta(x)\,\delta(y). \quad (10)$$

The term ΛC represents processes in which a certain proportion of the amount of the radionuclide is removed constantly from the cycle.

To solve the equatoin, we first eliminate the term ΛC by replacing C by $f = Ce^{-\Lambda t}$. The governing equation becomes

$$\frac{\partial f}{\partial t} + v_i \frac{\partial}{\partial x_i} f = \delta(t)\,\delta(x)\,\delta(y). \quad (11)$$

We use the mean quantity (with regard to the randomness of v) $\langle f \rangle$ and fluctuation from that, f'.

$$\frac{\partial \langle f \rangle}{\partial t} + \frac{\partial}{\partial x_i} \langle v_i f' \rangle = \delta(t)\,\delta(x)\,\delta(y). \quad (12)$$

After some approximation (see Hatano and Hatano, 1997), we obtain a macroscopic diffusion equation:

$$\frac{\partial \langle f \rangle}{\partial t} - D(t) \nabla^2 \langle f \rangle = \delta(t)\,\delta(x)\,\delta(y). \quad (13)$$

Random wind causes the particles diffuse in the free atmosphere like the Brownian motion. The solution gives the power law Eq. (2).

References

Chamberlain, A.C. (1970): Interception and retention of radioactive aerosols by vegetation. *Atmos. Environ.*, 4: 57-78.

Chappell, A. (1996): Modelling the spatial variation of processes in the redistribution of soil: Digital terrain models and in southwest Niger. *Geomorphology*, 17: 249-261.

Garger, E.K. (1994): Air concentrations of radionuclides in the vicinity of Chernobyl and the effect of resuspension. *J. Aerosol Sci.*, 25: 745-753.

Garger, E.K., Kashpur, V.A., Gurgula, B.I., Paretzke, H.G. and Tschiersch, J. (1994): Statistical characteristics of the activity concentration in the surface layer of the atmosphere in the 30 km zone of Chernobyl. *J. Aerosol Sci.*, 25: 767-777.

Garger, E.K., Hoffman, F.O. and Thiessen, K.M. (1997): Uncertainty of the long-term resuspension factor. *Atmos. Environ.*, 31: 1647-1656.

Garland, J.A., Pattenden, N.J. and Playford, K. (1991): *Resuspension Following Chernobyl.* Expert reviews of the modeling of resuspension, seasonality and losses during food processing. IAEA-TECDOC-647, Vienna, Austria.

Gifford F.A. (1991): The structure of atmospheric diffusion at regional scales. *U. S. Army Research Office, Final Technical Report, Contract No. P-027096-GS-S.*

Hatano, Y. and Hatano, N. (1997): Fractal fluctuation of aerosol concentration near Chernobyl. *Atmos. Environ.*, 31: 2297-2303.

Hatano, Y., Hatano, N. and Suzuki, A. (1995): Dynamic analysis of nuclide diffusion with illitization of the buffer material. *Waste Management*, 16: 495-500.

Hatano, Y., Hatano, N., Amano, H., Ueno, T., Sukhoruchkin, A.K. and Kazakov, S.V. (1998a): Aerosol migraion near Chernobyl: Long-term data and modeling. *Atmos. Environ.*, 32: 2587-2594.

Hatano, Y., Hatano, N., Barr, S. and Leck, C. (1998b): Turbulent transport of aerosols in the arctic marine surface layer, submitted.

Hoetzl, H., Rosner, G. and Wincler, R. (1992): Sources of present Chernobyl derived cesium concentrations in surface air and deposition samples. *The Science of Total Environment*, 119: 231-242.

Holländer, W. and Garger, E. eds. (1996): *Contamination of Surfaces by Resuspended Material: International Scientific Collaboration on the Consequences of the Chernobyl Accident (1991-1995).* section 4.3.1, European Commission, Belarus, Ukraine.

Kapoor, V. and Gelhar, L.W.(1994): Transport in three-dimensionally heterogeneous aquifers: 1. Dynamics of concentration fluctuations. *Water Resour. Res.*, 30: 1775-1788.

Lederer, C.M. and Shirley, V.S. eds. (1978): *Table of Isotopes, 7th ed.* John Wiley & Sons, New York.

Linsley, G.S. (1978): *Resuspension of the Transuranic Elements: A Review of Existing Data.* National Radiological Protection Board. Harwell, U.K.

Makhonko, K.P. (1992): Wind uplift of radioactive dust from the ground. *Atomic Energy*, **75**: 523-531.

Makse, A.H., Havlin, S., Schwartz, M. and Stanley, H.E. (1995): Method for generating long-range correlations for large systems. *Phys. Rev.*, **E53**: 5445-5449.

Monin, A.S. and Yaglom, A.M. (1975): *Statistical Fluid Mechanics: Mechanics of Turbulence.* (English edition) Vol. 2, section 21.4, 21.5 and 23.6, MIT Press, Cambridge, Massachusetts.

Nicholson, K.W. (1988): A review of particle resuspension. *Atmos. Environ.*, **22**: 2639-2651.

OECD/NEA (1995): *Chernobyl Ten Years on —Radiological and Health Impact.* OECD, Paris.

Watanabe, M., Amano, H., Ueno, T., Matsunaga, T., Nagao, S. and Onuma, Y. (1996): Study on migration behavior of radionuclides in the Chernobyl contaminated area (3) Specification of radionuclides in surface soil. *Presentation at Jpn. Soc. Health Phys. Meeting in May, 1996.*

Werner, B.T.(1995): Eolian dunes: Computer simulations and attractor interpretation. *Geology*, **23**: 1107-1110.

沙漠研究 10-3, 199-204 (2000)
Journal of Arid Land Studies

— Original Article —

Movement of Sand Dunes and its Prevention by Windbreaks at the Turpan Basin and the Taklimakan Desert in China

MAKI Taichi* and DU Mingyuan**

Meteorological observations and various kinds of investigations were carried out from 1990 to 1998 at the Turpan Basin, Xinjiang. This paper summarizes some of the findings of the studies made. The movement direction of sand dunes was from E to ESE. The average movement speed of sand dunes was 10.3 m per year. The average height of sand accumulation was 1.5 m in the case of a single tamarisk windbreak and 7.5 m on the first row and 1.5 m on the second row in the case of 2 rows of tamarisk windbreaks. The maximum height of sand accumulation for a half year was 40 cm and 30 cm in the cases of single windbreaks of 40% and 30% net densities, respectively. The effect of Japanese net windbreaks was higher than that of Chinese net windbreaks. The tamarisk is suitable for the marginal areas of arid lands. The results of the studies as well as discussions of greening, the effect of net windbreak at the Turpan Basin and the relation between the effect of net windbreaks and the protection of desert roads in the Taklimakan Desert were introduced and summarized here.

Key Words: Climate, Sand dune, Taklimakan, Turpan, Windbreaks, Wind erosion

1. Introduction

The authors reviewed and introduced information about the movement of sand dunes and the protection of land from sand dunes from the several original papers in the Journal of Arid Land Studies and the Journal of Agricultural Meteorology in Japan (Maki, *et al.*, 1993a, b, 1994, 1995; Maki, 1996, 1998).

Sand is supplied from dried up riverbeds, and reactivated old fixed and semi-fixed sand dunes. This is the most significant process of desertification. The desertification is not clear at gravel or pebble desert; gobi and stone or rock desert, but is much clear in sand desert areas or sand dune areas. In particular, agricultural fields, grasslands, shrub trees, roads, irrigation ditches and the like are buried by the sand movement in sand dune areas, and crops, animals and people's daily lives are affected significantly by drifting sand.

Sand dunes near the Turpan Desert Research Station were activated in recent years, *i.e.*, the risk of desertification was increasing and sand dunes were invading arable lands and settlements. The recent activity of transplanting trees is causing a rehabilitation near the Turpan Desert Research Station.

Some species of plants can grow in the severe environment of arid lands, but they have still to strong resistance character against drought, strong wind, heat, coldness and soil salinity. To mitigate the environmental severity, it is necessary to improve the climatic conditions in dry areas through the use of forest windbreaks, hedge windbreaks, net windbreaks and grass vegetation.

The most significant differences between the oases and the deserts are found in the air and soil temperatures. In

* Division of Agrometeorology, Department of Natural Resources, National Institute of Agro-Environmental Sciences, Ministry of Agriculture, Forestry and Fisheries. 3-1-1, Kannondai, Tsukuba, Ibaraki 305-8604, Japan.
Present address: College of Agriculture, Ehime University. 3-5-7, Tarumi, Matsuyama, Ehime 790-8566, Japan.
** Division of Agrometeorology, Department of Natural Resources, National Institute of Agro-Environmental Sciences, Ministry of Agriculture, Forestry and Fisheries. 3-1-1, Kannondai, Tsukuba, Ibaraki 305-8604, Japan.

(Received, June 19, 1999; Accepted, July 29, 1999)

oases, temperatures are lower in summer, higher in winter, lower at daytime and higher at nighttime. The ranges of annual and daily variations are smaller in oases than in the deserts. Average wind speeds in the oases are half in the deserts. Changes in air and soil temperatures after rainfall are more rapid in the deserts. Changes in the oases are slower because of greater soil moisture and humidity, so the rate of climatic alleviation is faster.

2. Characteristics of the desertification areas in the Turpan Basin

The sand dune areas near the Turpan Desert Research Station were desertified in resent years. The active sand dunes with the steep slope of 33 to 35 degrees on the leeward side of sand dunes were about 10 in 1990. Heights of these sand dunes were from 3 to 8 m, and the length of the largest sand dune with steep slope was 150 m. The sandy area of desert was 10 km^2 with 2 km of north-south and 5 km east-west distances, and the desert supplied sands on the windward side of observation area was 60 km^2, *i.e.*, a little sandy area and wind erosion area with bare clay soil. Therefore, the sand dunes are located on the leeward side of the above mentioned area due to the frequent wind direction of the strong wind. The activity of sand dune is decreasing at some parts of the transplanting near the Station and active sand dunes of 10 in 1990 is decreasing to almost nothing in 1996, but it is not sufficient to recover until now (Maki *et al.*, 1993a).

The observations on the relation among the distance of sand movement, duration of strong wind speed, and direction of strong winds were carried out on the sand dunes at 2 to 3 km from the Station. The largest sand dune of barchan type with 7 m in height near the Station was selected for observation (Maki *et al.*, 1995).

3. Moving direction and speed of sand dunes in the Turpan Basin

1) Relation between sand dune movement and meteorological elements

The annual prevailing wind direction at the Turpan Station is NE; however, the most frequent wind direction of strong winds over 17.2 m/s is W with a frequency of 49%, and the second-most frequent direction is WNW with frequency of 38%.

A wind speed of 8 m/s at 6 m height above the sand surface is equivalent to that of 6 m/s at 1 m. Movement of light sand particles begins from 5 m/s at 1 m height, but meanly from 6 m/s. The effect of wind around 5 to 6 m/s on sand movement is small, but that over 10 m/s is large (Maki *et al.*, 1995). The relations between blowing duration (t, hr) of the wind speeds over 5, 10 and 15 m/s and moving distance (d, m) of sand dunes, obtained from the observed results from Sep. 1, 1991, to Aug. 31, 1992, are expressed by the following equations.

$$d_5 = 0.0177 t_5 \quad (1)$$

$$d_{10} = 0.0687 t_{10} \quad (2)$$

$$d_{15} = 1.125 t_{15} \quad (3)$$

The proportional coefficient, k, of 0.0177 and wind speed (u, m/s) are expressed by the power relation with a correlation coefficient, r, of 0.918.

$$k = 4.63 \times 10^{-5} u^{3.38} \quad (4)$$

A similar relation was found for another period. The mean of the power values was 3.18, with the high correlation coefficient, r, of 0.952.

The relation among d, t and u is expressed by the following equation.

$$d = 7.3 \times 10^{-5} t \times u^{3.18} \quad (5)$$

Sand dunes move in proportion to the 3 powers of wind speed. The duration of strong winds from 8 to 10 m/s corresponds significantly to the moving distance of a sand dune. supposing 3 powers of time duration, t, in Eqs. (1), (2) and (3), the values of d are expressed as volumes (m^3) of sand, then these equations agree dimensionally with Eq. (5).

The correlation coefficient decreases in the case of a long period, because the volume of sand movement decreases in the case of reverse wind direction.

2) Moving direction and speed of sand dunes

The monthly moving directions and distances of sand dunes were expressed by vector as shown in Fig. 1, summarizing for one and half year of May 1991 to Oct. 1992. The moving distance was 9.0 m for a year from September 1991 to August 1992. The sand dune moves actually as a middle of E and ESE by the most frequent wind direction of strong winds from W to WNW.

The moving distance of 7 m-high sand dune was 9.5, 9.0, 12.0, 11.0, 10.0 and 10.0 m for each one year from

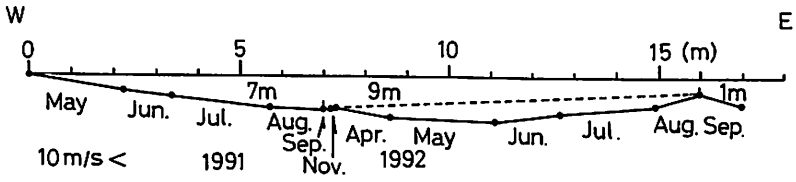

Fig. 1. Moving direction of sand dunes at the Turpan Station from April 1991 to December 1992. Wind speed over 10 m/s.

August to July for 6 years from 1990 to 1996, respectively, and the average was 10.3 m.

4. Effects of forest and net windbreaks on wind speed and sand movement

1) Effect of forest windbreaks at the Turpan Basin on wind erosion and sand accumulation

(1) Sand accumulation based on a single-row tamarisk windbreak

The height, width and forest density of a single-row tamarisk windbreak were 4.6 m, 12 m and 85%, respectively. Changes in the amount of sand accumulation in August 1991 are shown in Fig. 2. The high, medium and low sand accumulation heights for a long period of time at the center of the windbreak were 2.5, 1.5 and 0.5 m from spot to spot, respectively. Because wind erosion was minimal, sand accumulation took the values ranging from -6 H to 6 H. The values indicate the multiple distances of windbreak height, where a negative sign of H indicates the windward direction and a positive sign the leeward direction to the most frequent strong winds over 10 m/s from W to WNW or to the rather high wind of 5 to 10 m/s.

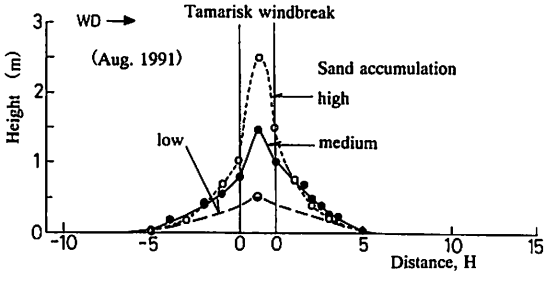

Fig. 2. Variations of sand accumulation effected by a single tamarisk windbreak.
WD: Wind direction

(2) Sand accumulation affected by two rows of tamarisk windbreaks

The tree heights, total heights and widths of two rows of tamarisk windbreaks were 2.5 and 4.0 m, 10.0 and 5.5 m, and 19 and 13 m for the first and second windbreaks, respectively. The forest densities of the windbreaks were 50% in the higher level and 100% in the middle to lower levels. Sand accumulation is shown in Fig. 3. The height of high, medium and low sand accumulation in the case of strong winds from W to WNW by the first wide windbreak was 8.0 m, 7.5 m and 6.5 m, respectively. In the case of the second narrow windbreak, the mean height of sand accumulation was 1.5 m at the central point and 2.5 m above the level of the irrigation ditch on the leeward side.

(3) Sand accumulation by two kinds of single row windbreaks

Net densities of two kinds of net windbreaks were 40 % (original 30 %) for A net and 45 % (original 40 %) for B net with the height of 2 m from November 1990 to May 1991 shown in Fig. 4. Sand accumulated at the region from -5 H to 12 H. The sand accumulation of 40 cm for B net was higher than that of 30 cm for A net at 3 H leeward side for 6-month term, and sand did not accumulate just under the nets based on the open space of 5 cm by relatively strong wind.

2) Example of greening at the Turpan Basin

Young trees of tamarisk (*Tamarix* L.), *Haloxylon ammodendron* Bge. and *Calligonum mongolicum* Turcz. with 20 to 30 cm in height and 1 cm in diameter of trunks are transplanted at the sandy or clay soil area near the Station in every winter. The rate of rooting is 10 to 70% depending on where the tree is planted. Seeds of *Capparis spinosa* L. Sp., which creeps on the ground surface are generally sowed, and irrigation is done for a small area only in winter season, using surplus water. As the

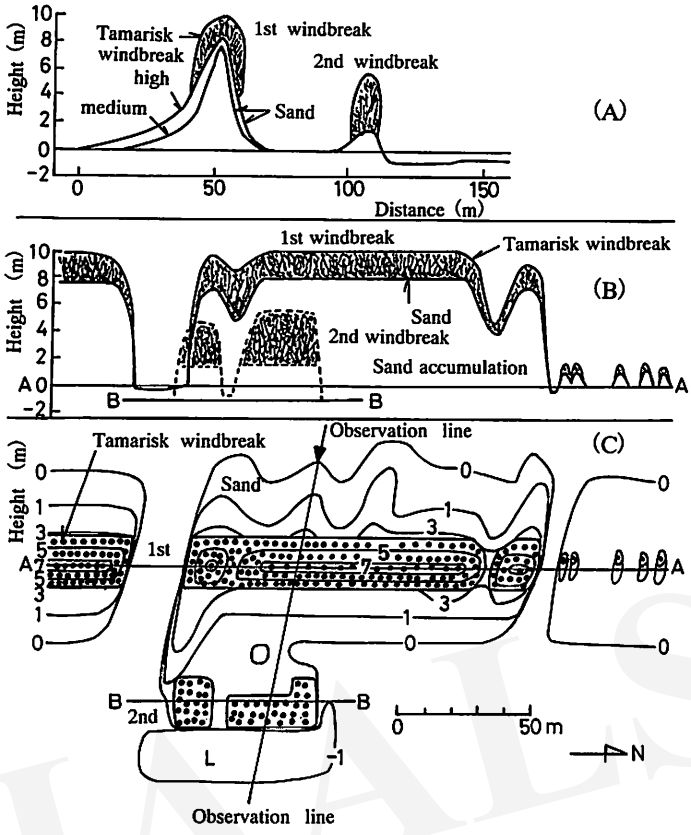

Fig. 3. Variations of sand accumulation effected by two rows of tamarisk windbreaks in transverse section (A), lateral view (B) and plane view (C).

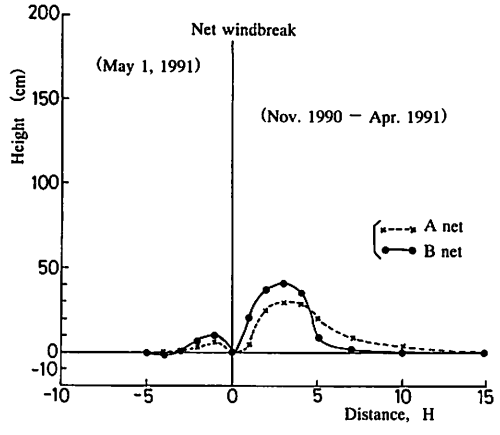

Fig. 4. Variations of sand accumulation induced by two kinds of single net windbreaks.

water freezes in winter, plants can use the water in spring when the ice melts. If the irrigation water is sufficient, poplars are transplanted along the road. Poplar (*Populus alba* L.) is common and is often transplanted in 1 or 2 high-density rows along roadsides.

At the Turpan Basin being representative of arid area in Northwest China, windbreaks are mainly *Populus alba* L. (poplar), *Tamarix* L. (tamarisk), *Ulmus pumila* L. Sp. (elm), *Salix* L. (willow), *Haloxylon ammodendron* Bge., *Calligonum mongolicum* Turcz., *Populus euphratica* Olivier. and *Elaeagnus angustifolia* L. Sp. Tamarisks have small leaves and stems with high-density growth of stems and leaves. It has a strong effect on wind decrease and it grows first if it is buried by sands. Tamarisks are suitable for the marginal areas of arid land because of their tolerance against wind, drought, heat, coldness and salinity (Makil *et al.*, 1993a, 1994).

3) Test desert road in the Taklimakan Desert and the effect of a net windbreak

An experiment was done along the test desert road constructed in the Taklimakan Desert for development of oil well stations from 1992 to 1995, because it was necessary to establish countermeasures against sand erosion and sand accumulation due to strong winds. The effects of forest windbreaks and net windbreaks were tested. The experiments of net windbreaks offered by the authors and hedge windbreak, and of test roads with brick, concrete, asphalt, salt mixture and the like, were mainly done by researchers of the Chinese Academy of Sciences along 2 km of the test road 100 km south of Luntai in the northern part of the Taklimakan Desert.

Decreases of wind speed and sand movement were measured at three kinds of test place: (a) straw-mat networks of 10 to 20 cm height of 1×1 m grid, 100 m wide and 2 km long; (b) hedge windbreaks of 1 to 2 m height made of reed straw and (c) net windbreaks of 2 m height made of plastic net. The desert road crossing the Taklimakan Desert in the north-south direction was constructed in 1996 after taking into consideration the results mentioned above.

According to the results of authors' observation using net windbreaks in the Taklimakan Desert, the effect was physically and meteorologically recognized to be similar to that at Turpan. One of the authors discovered that the effect of net windbreaks made in Japan with polyethylene Russell net of 2 mm mesh, 30 to 40% net density, 2 m height and 100 m length was higher than the effect of the net windbreak made in China with about 50% net density and 2 m height (Maki, 1996). The Japanese net was made of fine string and gave a relatively higher protection from the wind, although it allowed for higher ventilation due to its higher porosity. The Japanese net was not buried as much and suffered less damage. As it was found that the differences were significant, the Japanese net was used in a 1 to 2 km test area as a next step of practice. The results showed that it was also effective.

5. Conclusions

(1) Relation between movement direction and speed of sand dunes and climatic parameters were made clear, *i.e.*, sand dunes move in proportion to the 3 powers of wind speed, movement direction of sand dunes was from E to ESE and average movement speed of sand dunes was 10.3 m per year.

(2) Effects of several forest and net windbreaks on wind erosion and sand accumulation were estimated. The average height of sand accumulation was 1.5 m with the range of 2.5 to 0.5 m in the case of a single tamarisk windbreak, and was 7.5 m with the range of 8.0 m to 6.5 m on the first row and 1.5 m on the second row in the case of 2 rows of tamarisk windbreaks. The maximum height of sand accumulation for a half year was 40 to 30 cm in the cases of single windbreaks of 40 and 30 % net densities, respectively.

(3) Higher prevention of sand movement by windbreaks in the deserts of the Turpan Basin and the Taklimakan Desert were evaluated. The effect of Japanese net windbreaks was higher than that of Chinese net windbreaks. The tamarisk is suitable for the marginal areas of arid land, but the others, *i.e.*, poplar, elm, willow etc. are suitable for the irrigated area.

References

Maki, T. (1996): *Desertification and Greening in China and Food Crisis*. Shinzansha, 191pp. (in Japanese)

Maki, T. (1998): *Greening of Deserts*. Mediafactory, 128pp. (in Japanese)

Maki, T., Nakai, S., Takahata, S., Kitamura, Y. and Tohyama, M. (1993a): *The Front of Desert Greening*. Shinnihon Shuppan, 214pp. (in Japanese)

Maki, T., Pan, B., Du, M. and Uemura, K. (1993b): Meteorological improvement and prevention of drifting sand by net windbreak at dry land of Turpan in China. *J. Agr.* Met., 49: 159-167.

Maki, T., Pan, B., Du, M. and Uemura, K. (1994): Effects of double line windbreaks on the microclimate, sand accumulation and crop at the arid land in Turpan, China. *J. Agr.* Met., 49: 247-255.

Maki, T., Pan, B., Du, M. and Sameshima, R. (1995): Relation between desert climate and movement of sand dunes particularly at Turpan in Xinjiang of Northwest China. *J. Arid Land Studies*, 4: 91-101.

沙漠研究 10-3, 199-204 (2000)
Journal of Arid Land Studies

—原著論文—

中国のトルファンとタクラマカンの砂丘移動と防風施設による防砂

真木太一*・杜　明遠**

著者らは1990～1998年に中国新疆トルファンを中心に気象観測および各種調査を実施した．本報告では原著論文の中の興味深い観測結果の幾つかの事例を紹介する．トルファンの砂丘の移動方向はE～ESEであり，砂丘の年平均移動速度は10.3mであった．1列のタマリスク防風林による平均堆砂高度は1.5mであり，2列のタマリスク防風林の平均堆砂高度は1列目で7.5m，2列目で1.5mであった．密閉度40％と30％の1列の防風ネットによる半年間の堆砂高度はそれぞれ，40cmと30cmであった．日本製の防風ネットは中国製のものより保護効果が高かった．タマリスクは乾燥地の境界域に適する樹種である．その他，トルファン盆地における緑化事例と防風ネットによる効果事例，およびタクラマカン沙漠の道路保護と防風ネットの効果との関係を紹介した．

* 農林水産省農業環境技術研究所環境資源部気象管理科．現在：愛媛大学農学部
** 農林水産省農業環境技術研究所環境資源部気象管理科

(1999年6月19日受付；1999年7月29日受理)

沙漠研究 10-3, 205-214 (2000)
Journal of Arid Land Studies

—原著論文—

山形県山形市および鶴岡市における乾性降下物の化学組成

田中俊平*・柳澤文孝*・小谷　卓**

1．はじめに

日本各地で酸性雨が観測されているが，酸性雨の原因物質は硫黄酸化物や窒素酸化物などの大気汚染物質である．日本は，冬季から春季の季節風が卓越する時期に大陸の風下となることから，東アジアの都市部地域で発生した大気汚染物質が日本まで輸送されていると考えられている．

大日方・柳澤（1996）およびYanagisawa *et al.*(1997)は，山形の湿性・乾性降下物に含まれている非海塩性硫酸イオンのイオウ同位体比の季節変化について検討した．その結果，山形の乾性降下物に含まれている非海塩性硫酸イオンのイオウ同位体比は年間を通じてほとんど変化しないことから，現地性のイオウ分の影響が卓越していると結論した．また，大日方ほか（1998）は，日本海に面した鶴岡と内陸の山形で乾性降下物を採取してイオウ同位体比を測定し以下の諸点を明らかにした．

(1) 鶴岡の硫酸イオンと非海塩性硫酸イオンの降下量は山形のおよそ2倍である．また，山形において硫酸イオンと非海塩性硫酸イオンの降下量には明確な季節変化は見られないが，鶴岡では冬季と春季に降下量が増加する．

(2) 山形の乾性降下物に含まれている非海塩性硫酸イオンのイオウ同位体比は年間を通じて＋4～＋5パーミルで推移していることから，現地性のイオウ化合物が卓越している．

(3) 鶴岡の非海塩性硫酸イオンのイオウ同位体比は，夏季～秋季は＋2～3パーミル，冬季～春季は＋5～＋8パーミルで推移しており，季節変動が認められる．

(4) 鶴岡では夏季～秋季に弱い東風が吹くことが多いことから夏季～秋季の値は現地性の非海塩性硫酸イオンの同位体比と考えられる．

(5) 冬季に鶴岡に降下する非海塩性硫酸イオンは大陸北部で産した石炭起源のイオウ酸化物が北西季節風に乗って運ばれてきた可能性が考えられる．

(6) 鶴岡の春季のイオウ同位体比は黄砂の影響と考えられる．

これらのことは，両地域でイオウ同位体比の挙動に差異があることを意味するものである．

本研究では日本海側の鶴岡市および内陸の山形市で採取した乾性降下物に含まれている主要成分（ナトリウムイオン・カリウムイオン・マグネシウムイオン・非海塩性カルシウムイオン・塩化物イオン・硝酸イオン・非海塩性硫酸イオン）と微量成分（亜鉛・鉛）の分析を行った．また，山形県環境保全センター（1993-1999）の行っているイオウ酸化物（SO_2）と窒素酸化物（$NO+NO_2$）の大気環境測定結果，および，降下煤塵の測定結果との比較を行い成分の起源について考察した．

2．試料採取

山形県の鶴岡市にある鶴岡工業高等専門学校と山形市にある山形大学理学部の屋上で採取した（Fig. 1）．乾性降下物は柴田科学製ハイボリウムエアサンプラーHVC-1000A型を用い1分間700リッターの流量で大気を吸引した．試料採取は216時間の休止期間をはさみ120時間運転する方法で行った．採取期間は1993年10月から1998年6月までである．なお，鶴岡では1993年12月24日から1994年3月2日までエアサンプラー故障のため試料採取できなかった．また，フィルターには東洋濾紙社製QR100石英繊維フィルター（253×203 mm）を使用した．

3．分析方法

1）水抽出方法

フィルターの4分の1を分析に用いた．フィルターをハサミで細断してガラスビーカーに入れ，蒸留水20mlを加えて5分間超音波洗浄器にかけ可溶性成分を抽出し

*山形大学理学部地球環境学科
**鶴岡工業高等専門学校

(1999年7月26日受付；1999年11月2日受理)

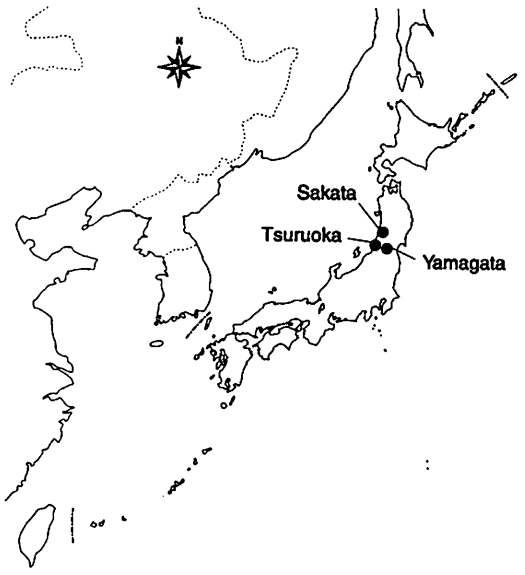

Fig. 1. Location of aerosol sampling stations.

た．この操作を5回繰り返し，各浸出液を合わせてから1 μmのMillipore社製メンブランフィルターで濾過し一定容とした．陰イオン（硫酸イオン・硝酸イオン・塩化物イオン）と陽イオン（ナトリウムイオン・カリウムイオン・マグネシウムイオン・カルシウムイオン）を分析した．

2）酸抽出方法

フィルターの8分の1を分析に用いた．フィルターをハサミで細断してガラスビーカーに入れ，環境庁大気保全局の大気汚染物質測定法指針（環境庁大気保全局，1988）に従って，1＋1のHCl 30mlおよび30％のH_2O_2 5 mlを加えて水浴上で30分間加熱抽出した．その溶液を1μmのMillipore社製メンブランフィルターで濾過した後，ホットプレート上で加熱濃縮し，1＋9 HClを加えて一定容として鉛イオン・亜鉛イオンを分析した．

3）分析方法

陰イオン（硫酸イオン・硝酸イオン・塩化物イオン）はDIONEX社製2020i型イオンクロマトグラフィーによって，陽イオン（ナトリウムイオン・カリウムイオン・マグネシウムイオン・カルシウムイオン・鉛イオン・亜鉛イオン）はセイコー電子工業株式会社製SPS7000A型発光分光分析装置を用いて定量した．

4）海塩粒子補正

日本は四方を海に囲まれていることから海塩粒子の影響を無視するわけにはいかない．非海塩性硫酸イオン濃度（SO_4^{2-}nss），および，非海塩製カルシウムイオン濃度（Ca^{2+}nss）は測定したナトリウムイオンが全て海塩粒子起源であると仮定して海水中の存在比から下式によって算出した．

$$SO_4^{2-}nss = SO_4^{2-}mes - (SO_4^{2-}sea/Na^{+}sea) \times Na^{+}mes$$

$$Ca^{2+}nss = Ca^{2+}mes - (Ca^{2+}sea/Na^{+}sea) \times Na^{+}mes$$

ここで，SO_4^{2-}mes，SO_4^{2-}sea，Na^{+}mes，Na^{+}sea，Ca^{2+}mes，Ca^{2+}seaはそれぞれ，試料の硫酸イオン濃度，海水の硫酸イオン濃度，試料のナトリウムイオン濃度，海水のナトリウムイオン濃度，試料のカルシウムイオン濃度，海水のカルシウムイオン濃度である．なお，海水中の存在比はSO_4^{2-}sea/Na^{+}sea比，および，Ca^{2+}sea/Na^{+}sea比それぞれ0.252と0.0384である．

4．結果と考察

1）ナトリウムイオン・カリウムイオン，マグネシウムイオン，塩化物イオン

ナトリウムイオン・カリウムイオン，マグネシウムイオン，塩化物イオンは海塩粒子成分である．Fig. 2にナトリウムイオンの季節変化を示した．黒丸（●）が山形，白丸（○）が鶴岡である．ナトリウムイオン濃度は年間を通じて鶴岡の方が山形に比べて常に高くなっており，両地域とも冬季に濃度が上昇している．図示しなかったが，他の海塩粒子成分（カリウムイオン，マグネシウムイオン，塩化物イオン）もナトリウムイオンと同様の挙動を示しており，また，各海塩粒子成分の降下量は互いに相関関係があることが認められる．これらのことは，海塩粒子成分が冬季に卓越する北西の季節風によって供給されたものであり，海により近い鶴岡の方が海塩粒子の影響が強いという地理的要因を反映していると考えることができる．

2）硝酸イオン・非海塩性硫酸イオン

硝酸イオンは山形・鶴岡両地域ともに冬季に濃度の上昇する季節変化が見られた（Fig. 3）．対流圏における窒素酸化物の収支についてWHO（1997）が報告している．それによると大気中の窒素酸化物は化石燃料やバイオマスの燃焼の際に大気中の窒素が酸化されることによって生成されるものが多いと見積もっている．また，大気中

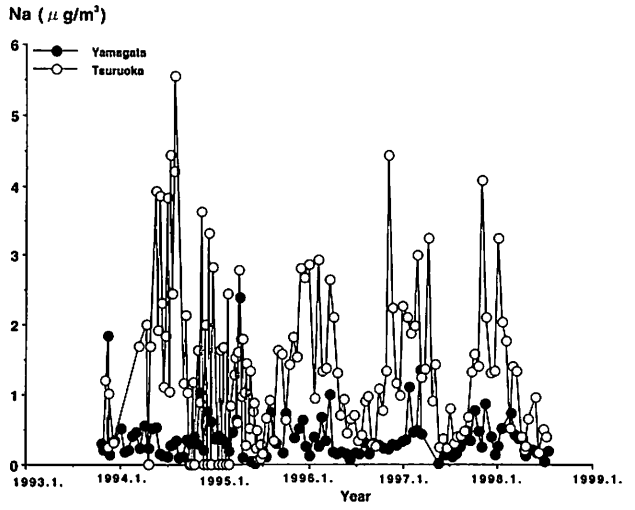

Fig. 2. Seasonal variation of sodium deposition rate ($\mu g/m^3$) in dry deposition in Yamagata (●) and Tsuruoka (○).

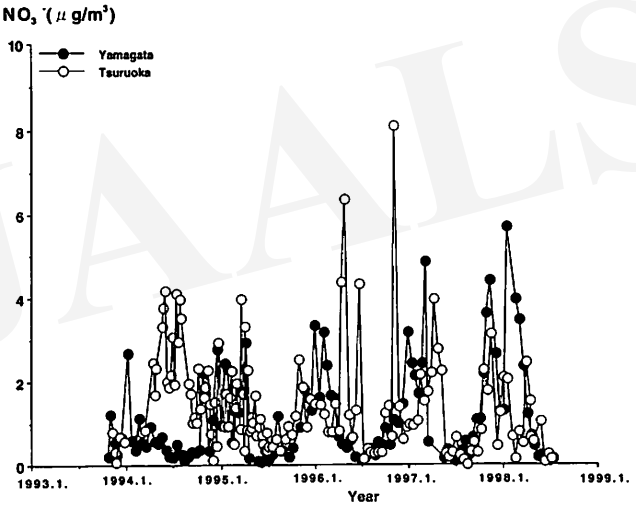

Fig. 3. Seasonal variation of nitric acid deposition rate ($\mu g/m^3$) in dry deposition in Yamagata (●)and Tsuruoka (○).

に供給された窒素酸化物は乾性沈着と湿性沈着によって除去されるとしている．

山形県環境保全センター（1993-1999）は大気中の窒素酸化物（$NO+NO_2$）について山形と鶴岡で測定を行っている．それによると，大気中の窒素酸化物の濃度は（Fig. 4）山形・鶴岡ともに冬季に濃度が高くなる季節変化が見られた．しかし，濃度は山形の方が常に高く，また，鶴岡で観測された濃度変動の幅は山形に比べて小さいものであった．水野ほか（1990）は冬期に地面が冷却される気象条件の下で大気浮遊物質や窒素酸化物が高濃度になる現象を報告している．さらに，神奈川県公害防止推進協議会の環境濃度解析調査（神奈川県公害防止推進協議会, 1994）によると，冬季は一般に季節風が支配的であるため風速による希釈効果が高く，濃度が高くなるのは風の弱い日に限られており，また，地上付近の発生源影響が主流と考えられると報告している．これらのことを考慮すると，山形では冬季になると地面が冷却されるとともに盆地地形で風が弱いことから山形盆地内にガス状物質が拡散せずに滞留してしまうことで窒素酸化物の濃度が高くなっていると考えることができる．一

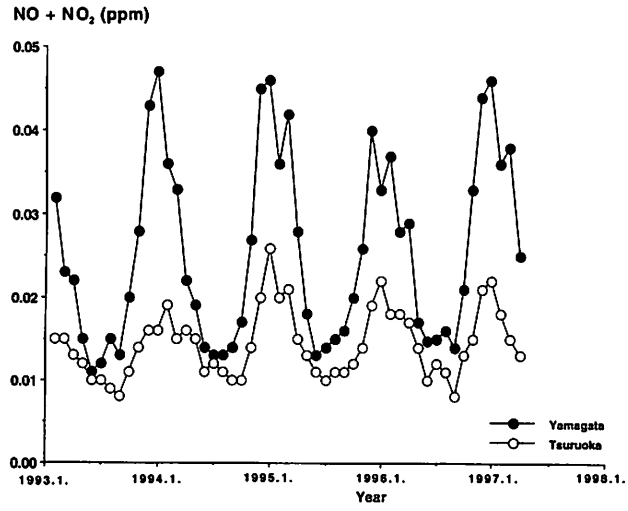

Fig. 4. Seasonal variation of ($NO+NO_2$) concentration (ppm) of in atmosphere in Yamagata (●) and Tsuruoka (○).

方，鶴岡でも地面は冷却されるが，北西季節風が卓越する平野部に位置することから風によって拡散されているために窒素酸化物が低濃度となっていると推定される．

さて，大気中の窒素酸化物（$NO+NO_2$）の濃度は毎年冬季にピークを示す季節変動を示している．一方，乾性降下物に含まれている硝酸イオンの濃度も冬季に高くなる季節変動を示している．従って，乾性降下物に含まれている硝酸イオンの挙動は，前駆物質である窒素酸化物の挙動を反映したものと推定される．しかし，両者を詳細に比較すると，大気中の窒素酸化物の濃度は1月付近でピークとなるが乾性降下物に含まれている硝酸イオンの濃度は必ずしも1月にピークを示すわけではない．また，1994年の鶴岡では夏季にピークが存在する．このように大気中の窒素酸化物濃度と乾性降下物に含まれている硝酸イオンの濃度の変動は必ずしも一致するわけではない．化石燃料やバイオマスの燃焼起源以外の大気中の窒素酸化物の起源として，特に鶴岡のように海岸に面した地域では海からの影響を考慮する必要があるだろう．本研究では大気中の窒素酸化物濃度は1カ月間の，乾性降下物に含まれている硝酸イオン濃度は5日間の平均値である．両者の相関を論じるにはより短い期間に窒素酸化物と乾性降下物を同時に採取して濃度変化の類似性を比較する必要がある．

一方，非海塩性硫酸イオンは鶴岡の方が濃度が高いが，山形でも鶴岡でも明確な季節変化は認められなかった（Fig. 5）．非海塩性硫酸イオンは，主に化石燃料の燃焼によって生じるイオウ酸化物を起源とするものである．非海塩性硫酸イオンの前駆物質であるイオウ酸化物（SO_2）についての山形県環境保全センター（1993-1999）の大気環境測定結果によると，イオウ酸化物は山形で冬季に濃度が高くなる季節変化が見られたが，鶴岡では明瞭な季節変化は見られなかった（Fig. 6）．窒素酸化物と同様に，山形では冬季になると地面が冷却されるとともに風が弱いことからガス状物質が拡散させずに滞留してしまうことでイオウ酸化物の濃度が高くなっている．一方，鶴岡では風によって拡散されているためにイオウ酸化物が低濃度となっていると考えることができる．しかし，イオウ酸化物の挙動は乾性降下物に含まれている非海塩性硫酸イオンと異なっており，非海塩性硫酸イオンの挙動がイオウ酸化物の挙動を反映したものであると考えることはできない．

大日方ほか（1998）は鶴岡と山形で乾性降下物を採取してイオウ同位体比を測定し，以下の諸点を明らかにしている．山形の乾性降下物に含まれている非海塩性硫酸イオンのイオウ同位体比は年間を通じて＋4～＋5パーミルで推移していることから，現地性のイオウ分化合物が卓越していると考えられる．これに対し，鶴岡の非海塩性硫酸イオンのイオウ同位体比は，夏季～秋季は＋2～3パーミル，冬季～春季は＋5～＋8パーミルで推移しており，季節変動が認められる．夏季～秋季の値は現地性の非海塩性硫酸イオンの同位体比と考えられるが，冬季は大陸北部で産した石炭起源のイオウ酸化物が，春季は黄砂の影響が考えられる．以上のことは，非海塩性硫酸イオンが移流してくる際にイオウ酸化物以外の形態

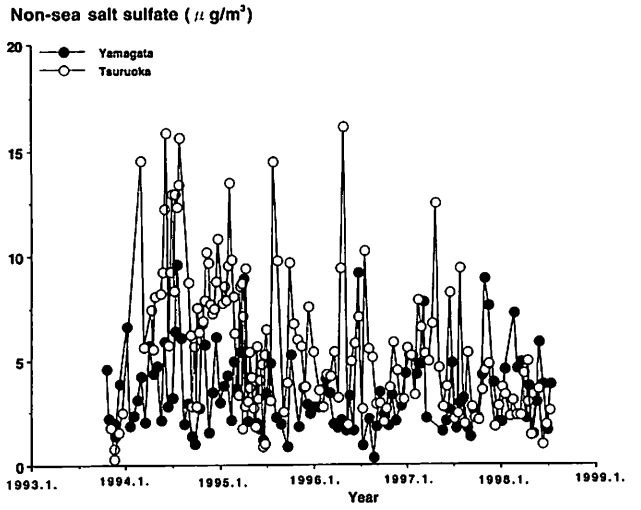

Fig. 5. Seasonal variation of non-sea salt sulfate deposition rate ($\mu g/m^3$) in dry deposition in Yamagata (●) and Tsuruoka (○).

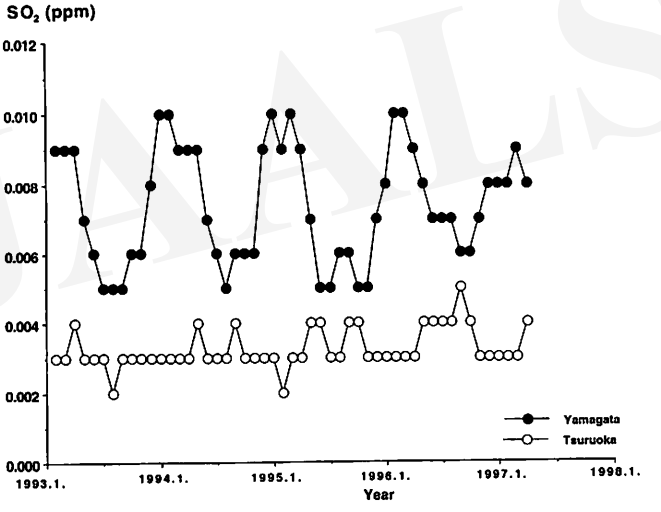

Fig. 6. Seasonal variation of SO_2 concentration (ppm) in atmosphere in Yamagata (●) and Tsuruoka (○).

でもたらされていることを示すと考えられる．この点については更に検討が必要である．

3）非海塩性カルシウムイオン

非海塩性カルシウムイオンの主な起源として土壌や表層堆積物・道路粉塵をあげることができる．山形県環境保全センター（1993-1999）は降下煤塵（t/km²/month）の測定を行っている（Fig. 7）．測定は山形と酒田で行われているが鶴岡では測定されていない．酒田と鶴岡はともに日本海に面した小都市であり直線距離で20kmほどしか離れていないことから条件は同じと考えられるので，以下の論議は酒田のデータを用いることにする．降下煤塵量は山形と酒田ともに冬から春にかけて濃度が上昇する顕著な季節変化が見られた．一方，山形と鶴岡で採取した非海塩性カルシウムイオン濃度は春季にやや上昇する季節変化が見られた（Fig. 8）が，変動は降下煤塵の場合と比較して顕著なものではない．従って，乾性降下物に含まれている非海塩性カルシウムイオンの挙動

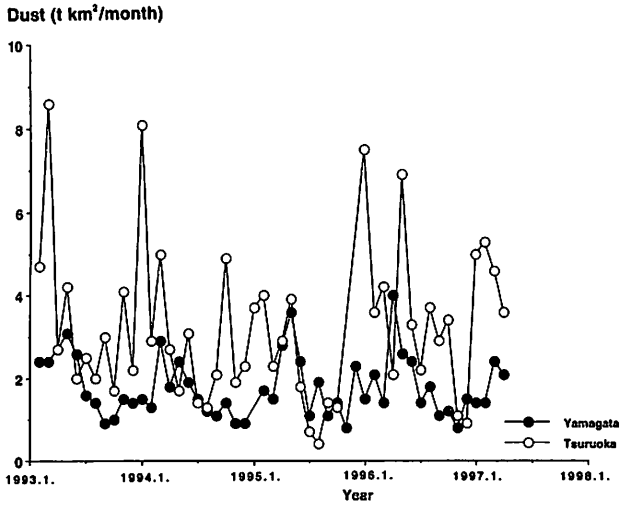

Fig. 7 Seasonal variation of dust deposition rate (t/km^2/month) in atmospere in Yamagata (●) and Sakata (○).

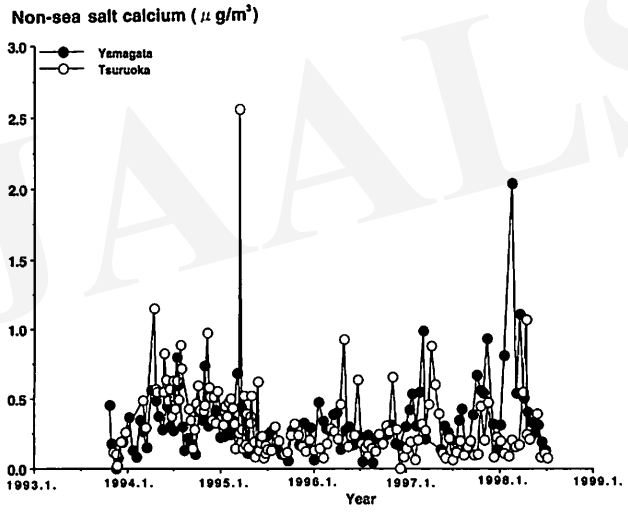

Fig. 8. Seasonal variation of non-sea salt calcium deposition rate (μg/m^3) in dry deposition in Yamagata (●) and Tsuruoka (○).

は道路粉塵の挙動を反映したものと断定することはできない．降下煤塵の主な起源は道路粉塵であり土壌や表層堆積物も含まれていると考えられる．各要因について個別に微量元素等の比較を行っていく必要がある．

なお，1998年3月末に非海塩性カルシウムイオン濃度が他に比べて高濃度になっている．この試料は山形で黄砂現象が肉眼で観測された1998年3月30日（山形地方気象台，1998）に採取された試料である．カルシウムイオンは大陸から飛来してくる黄砂にも含まれている成分でもある．このことから，1998年3月末は黄砂粒子の影響を受けて山形で非海塩性カルシウムイオンの濃度が上昇したと考えられる．なお，鶴岡ではこの時期に乾性降下物の採取は行われていない．一方，田中ほか（1998）によると山形および鶴岡で採取された乾性降下物に含まれている非海塩性カルシウムイオンとストロンチウムイオンの降下量に相関関係が認められること，$^{87}Sr/^{86}Sr$比が夏季に低下し冬季～春季にかけて上昇することなどから、冬季～春季に大陸の土壌起源物質の影響があること

を示唆している．乾性降下物に含まれている主要成分のデータだけでは黄砂からどの程度の影響を被っているか推定することは難しい．今後，様々な指標を用いて多面的に解析していく必要がある．

4）亜鉛・鉛

亜鉛の濃度（Fig. 9）は両地域でほぼ同様であるのに対して，鉛の濃度（Fig. 10）は年間を通じて鶴岡で高い値を示している．

向井ほか（1989），Hashimoto *et al.*（1990, 1991），関根・橋本（1991）は，日本各地と韓国で乾性降下物を採取して主要成分・微量成分の分析を行っている．この結果によると，日本のPb/Zn比は夏季では0.2～0.3であるが冬季に高く，同じ冬季でも西日本の方が東日本より値が高いと報告している．この要因として，韓国では有鉛ガソリンが使用されていることからPb/Zn比が高く0.8前後の値になるとしている．また，日本では無鉛ガソリンが使用されているためにPb/Zn比が低いが，大陸からの

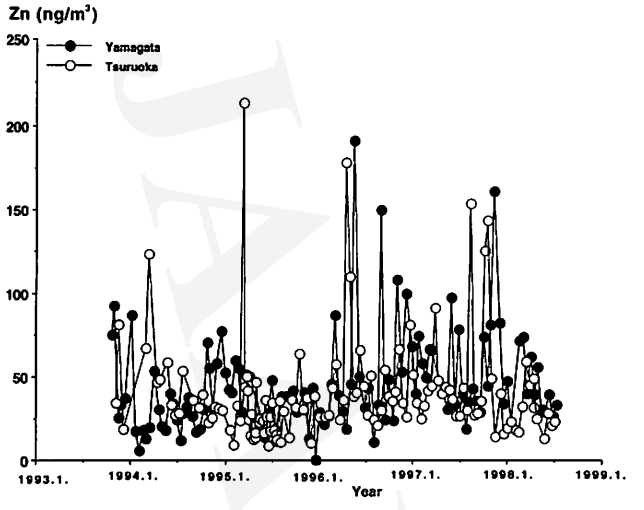

Fig. 9. Seasonal variation of zinc deposition rate (ng/m^3) in dry deposition in Yamagata (●) and Tsuruoka (○).

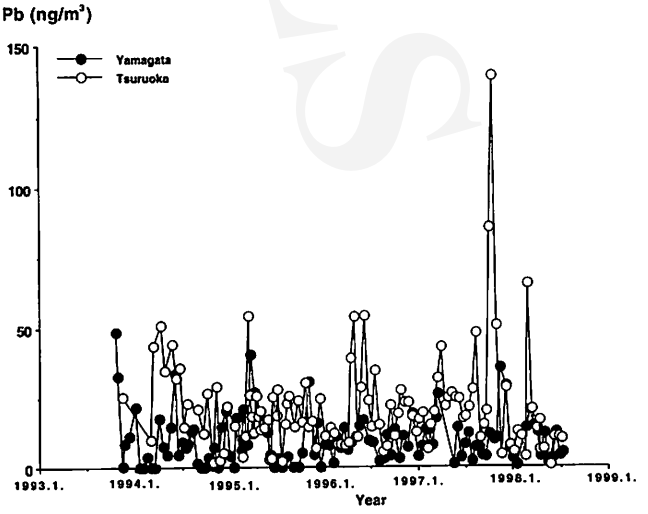

Fig. 10. Seasonal variation of lead deposition rate (ng/m^3) in dry deposition in Yamagata (●) and Tsuruoka (○).

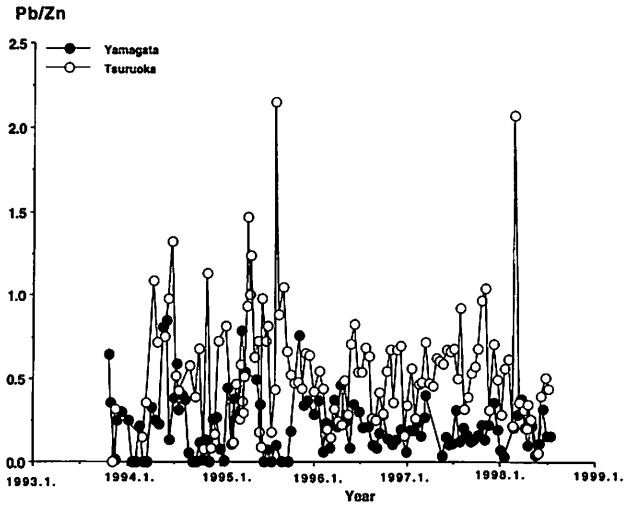

Fig. 11. Seasonal variation of lead-zinc ratio (Pb/Zn) in dry deposition in Yamagata (●) and Tsuruoka (○).

影響が大きい冬季や大陸の影響を受けやすい西日本では比率が高くなるとしている．山形における鉛・亜鉛比（Pb/Zn）は（Fig. 11）0.1～0.4の値で推移しているのに対し，鶴岡では0.2～0.8と山形より高い値である．また，山形のPb/Zn比はHashimoto *et al.* (1990, 1991)，関根・橋本（1991）が報告している日本国内の原地性の値とほぼ同じであるのに対して，鶴岡のPb/Zn比は西日本の冬季の値に近いものである．しかし，韓国ではガソリンの無鉛化がはかられたことから，現在でも韓国からの影響で日本の乾性降下物中のPb/Zn比が高くなるとは考えにくい．一方，中国では現在でも有鉛ガソリンが使用されていることから中国からの影響は考え得ることである．しかし，本研究では関根・橋本（1991）が指摘しているようなPb/Zn比の冬高夏低の季節変動を認めることはできなかった．これは，鶴岡では常にPb/Zn比の高いものが，一方，山形では常に低いものが供給されていることになる．このことは，鉛・亜鉛の起源について東アジア諸国の有鉛ガソリンだけではなく，試料採取地周辺の土壌や表層堆積物・海水等の影響も検討しなくてはならないことを示唆するものである．

5．結　論

(1) 海塩粒子成分の濃度は年間を通じて鶴岡の方が山形に比べて常に高くなっている．また，両地域とも冬季に濃度が上昇している．これらのことは，海塩粒子成分が冬季に卓越する北西の季節風によって供給されたものであり，海により近い鶴岡の方が海塩粒子の影響が強いという地理的要因を反映していると考えることができる．

(2) 硝酸イオンの濃度はともに冬季に濃度の上昇する季節変化が見られた．乾性降下物に含まれている硝酸イオンの挙動は前駆物質である窒素酸化物の挙動を反映した可能性が考えられる．

(3) 非海塩性硫酸イオンは鶴岡の方が濃度が高いが，山形でも鶴岡でも明確な季節変化は認められなかった．非海塩性硫酸イオンの挙動はイオウ酸化物の挙動を反映したものとはいえない．

(4) 非海塩性カルシウムイオンは山形と鶴岡ともに春季に濃度がやや上昇する季節変化が見られた．なお，山形県で黄砂現象が観測された1998年3月末に採取された試料に含まれているカルシウムイオン濃度は他に比べて高濃度であり，黄砂粒子の影響を受けたと推定される．

(5) 亜鉛の濃度は両地域でほぼ同様であるのに対して，鉛の濃度は鶴岡で年間を通じて高い値を示している．

謝　辞

乾性降下物の採取に際して，山形大学理学部地球環境学科の大日方　裕氏と伊藤　博氏と鶴岡工業高等専門学校の生徒さんたちのご協力を得た．記してお礼申し上げます．

引 用 文 献

神奈川県公害防止推進協議会 (1994):「「浮遊粒子状物質対策調査」報告書」

環境庁大気保全局 (1988):「大気汚染物質測定法指針」

水野建樹・近藤裕昭・松川宗夫 (1990): 関東平野において初冬に粉じんが極めて高濃度となる気象条件について.「大気汚染学会誌」**25** (2): 143-154.

向井人史・阿部喜也・椋　達則・竹下和男・福間常夫・高橋順一・溝田真司 (1989): 隠岐島における大気粉じん成分の長期的変動.「国立公害研究所研究報告」**123**: 7-50.

大日方　裕・柳澤文孝 (1996): 湿性・乾性降下物に含まれる硫酸イオンのイオウ同位体比.「月刊地球」号外 **16** (酒井　均教授退官記念号「新しい海洋化学の構築」): 182-186.

大日方　裕・柳澤文孝・小谷　卓・上田　晃 (1998): 山形県鶴岡市と山形市の乾性降下物に含まれている硫酸イオンのイオウ同位体比.「沙漠研究」**7**: 199-126.

関根嘉香・橋本芳一 (1991): 東アジア地域における粒子状大気汚染物質の長距離輸送.「大気汚染学会誌」**26**: 216-226.

田中真理子・柳澤文孝・矢吹貞代 (1998): 山形県におけるエアロゾル中のSr同位体比の季節変動.「理研シンポジウム「乾燥地起源の風送ダスト～発生・長距離輸送・環境影響～」講演要旨集」

山形地方気象台 (1998):「山形気象月報平成10年3月」

山形県環境保全センター (1993-1999):「大気環境測定結果」

Hashimoto, Y., Kim, H.-K., Otoshi, T. and Sekine, Y. (1990): Monitoring of atmosperic aerosol components by multi-elemental neutron activation analysis in Seoul, Korea, April 1987-March 1989. *J. Japan Soc. Air Pollut.*, **25**: 313-323.

Hashimoto, Y., Kim, H-K, Otoshi, T. and Sekine, Y. (1991): Air quality monitoring at Seoul, Korea－ May 1986-March 1989. *J. Japan Soc. Air Pollut.*, **26**: 51-58.

WHO (1997): *Nitrogen Oxides, 2nd Ed., Environmental Health Criteria 188.* The World Health Organization, pp.367.

Yanagisawa, F., Obinata, Y., Ueda, A. and Shida, J. (1997): Sulfate ion in atmospheric deposition in Japan. (1) Sulfur isotope ratios of sulfate in wet deposition in Japan. *Proc. Int. Cong. Acid Snow and Rain, Niigata*, 143-148.

沙漠研究 10-3, 205-214 (2000)
Journal of Arid Land Studies

— Original Article —

Chemical Composition of Dry Deposition in Tsuruoka and Yamagata, Yamagata Prefecture, Japan

TANAKA Shunpei*, YANAGISAWA Fumitaka* and KOTANI Takashi**

In order to investigate the origin of the atmospheric particulate matter, dry depositions were collected, using high volume air sampler, at two localities, Tsuruoka and Yamagata in Yamagata Prefecture, Japan, from 1993 to 1998. Tsuruoka locates at the Japan Sea coastal area and Yamagata locates in the basin, 80 km far from the coast of the Japan Sea. The deposition rates of water-soluble components (Na, K, Mg, Ca, SO_4, NO_3 and Cl) and acid-soluble components (Pb and Zn) in the dry depositions were investigated. Sea salts (Na, K, Mg and Cl) increases both in Yamagata and Tsuruoka in winter with the prevalence of the winter monsoon from Siberia, but the deposition rate in Tsuruoka is higher than that in Yamagata all through the year. Nitric acid in Yamagata and Tsuruoka is higher in winter and lower in summer, and agrees with seasonal variation of NOx in atmosphere. On the other hand, the seasonal change of non-sea salt sulfate is not observed. Non-sea salt calcium in Yamagata and Tsuruoka is higher both in winter and spring. The increase in spring is strongly related to the Kosa phenomenon observed in March 1998 at Yamagata. It means that Kosa could be another source of non-sea salt calcium. Though deposition rate of zinc that was observed in Yamagata and Tsuruoka is similar, deposition rate of lead in Tsuruoka was higher that in Yamagata.

Key Words: Chemical composition, Dry deposition, Yamagata, Tsuruoka, Kosa

* Department of Earth and Environmental Sciences, Faculty of Science, Yamagata University. 1-4-12, Kojirakawa, Yamagata 990-8560, Japan.

** Tsuruoka National College of Technology. 104, Sawada, Ioka, Tsuruoka 997-0842, Japan.

(Received, May 27, 1999; Accepted, November 12, 1999)

沙漠研究 10-3, 215-224 (2000)
Journal of Arid Land Studies

アルゼンチン乾燥地域の農業と水問題

高宮一喜*・筒井　暉**

1．まえがき

南米の砂漠というとエクアドルからペルー，チリの北部に長く続く，アンデス山脈西側の砂漠が一般的な概念であり，とりわけペルーの南部にあるナスカの地上絵は名高い．

一方アンデス山脈の東側は，ブラジルの大河アマゾンの水源地帯であり，多量の降雨に恵まれた緑濃い南米の大地を形成している．だが，東側においてもアルゼンチンのメンドーサを中心とする地域は年間雨量200mm以下の乾燥地帯であり，潅漑なしでは農業は成立しない．この乾燥地域ではアジア，アフリカのそれと同様，潅漑による土壌の塩類集積が問題となっており，都市の膨張に伴う上水の確保のため深刻な水争いが起こっている．

本文では，緑濃いパンパを想像されるアルゼンチンにおけるアンデス山脈以東の乾燥地域の農業と水問題を取り上げる．

2．アルゼンチン国とその農牧業の概況

1）土地利用

アルゼンチン国は，南米大陸の最南端，南緯22～55度，西経54～73度に位置し，南北の長さは約3,650km，東西の最大幅は1,700km，海岸線の総延長は約5,000kmで先端を南に向けた楔状の形をした国土を持つ（図1）．国土は大きく分けて，西部（アンデス地方），北部，中央部（パンパ地帯），南部（パタゴニア地方）の4地域にわけられる．西部はチリとの国境をなしているアンデス山脈地帯で，大西洋または太平洋に注ぐ（長さ約3,600km，河口の川幅が約90kmのラプラタ河に代表される）多くの河川の分水嶺となっている．また，この地域にはアコンカグア（標高7,023m）をはじめとする7,000m級の高峰がそびえ，南に下るにつれて低くなっている．

北部のアンデス山脈から南のパンパまで肥沃な森林地帯が広がり，雨量も多く，農業，牧畜業，林業の好適地である．この地域には，高さ80m，幅約4 km，毎秒1,750tの水量が落下する世界一のイグアス大瀑布がある．中央部はパンパと呼ばれる大平原地帯で，面積753,000 km^2（パンパ地帯はラ・パンパ州，ブエノス・アイレス州，サンタ・フェ州およびコルドバ州にわたる地帯），平坦かつ肥沃で，農業，牧畜が行われ，農業国アルゼンチンの富の源泉になっている．南部は起伏に富んだ半砂

図1．アルゼンチン国の行政区分．
Fig. 1. State of Argentina.

* 元FAOラテンアメリカ地域事務局，上級水管理専門官，緑公団嘱託
** 近畿大学農学部

(1999年9月24日受付；2000年5月17日受理)

漠地帯でパタゴニアと呼ばれ，常に強い西風が吹く不毛の地であるが，この国の重要な羊の産地であるとともに，石油資源地帯としてアルゼンチン国経済に大きな比重を占めている．

アルゼンチンにおける農業の国内総生産に占める割合は，1982年以降約15％～17％で推移している（1990年はGDPの16.7％）．特に国土の約1/4を占める湿潤パンパ地帯（約8,000万ha）での穀物（小麦，とうもろこし，大豆等），家畜（牛，馬，羊等）の生産量が国全体の経済に大きな影響を与えている．農林水産物の輸出は，その加工品を含めると総輸出額約123億ドル（1990）の5割以上を占める約68.7億ドルで最も重要な産業となっており，最近（1997）のデータでは純輸出額は倍増していて農林水産物の輸出は加工品を含めると約6割に増えている．

1991年には約169百万haが農用地として利用されている（表1）．このうち耕地は25,000千ha，永年作物が2,200千ha，牧草地が142,100千haである．農牧業経営体（1988）は421,221戸，農業就業人口（1992）は1,175千人で，全就業者の約9.9％を占めているが，最近減少傾向にある．1戸あたりの耕地面積（1974）は約400haとなっている．農用地はほとんどが牧草地で牧場経営規模は全体の約2/3を占める100ha以下の農家が耕地面積では5％程度なのに対し，全体の0.6％の10,000ha以上の農家が全面積の1/3を，また全体の2.7％の2,500ha以上の農家が全面積の60％を占めるという大土地所有制が残っている．これらは相続税がないという税法上の問題もあるが，大牧場主は通常ブエノス・アイレス都市部に居住しており，農村社会は小規模経営農家，農場労働者，ガウチョ（カウボーイ）などで形成されている．近年経済不況のため，その一部の都市への流出が起こっている．

パンパ地帯での農牧経営方法は，広大な経営面積の1/2～1/3程度を穀物栽培に当て，残りを放牧地として利用する輪作方式を基本にしている．肥料，農薬等の投入がほとんどいらないチェルノーゼムと呼ばれる肥沃な表土が1mほどあるうえ，十分余裕を持った土地利用が行えることから，非常に安価な農業経営が行われている．最近ではさらに低コストな不耕起農法が約50万haで行われており，土壌保全上は問題となっている（土壌保全法が1981年制定され補助金制度ができたが，1989年廃止されている）．

しかしながら，このような恵まれた経営体制と国民の必要量が簡単に生産でき，かつ輸入もできるという状況などから，歴史的に農牧業の基盤整備に対する投資は消極的で，比較的粗放な農業技術と相俟って，生産力にはまだ十分な余裕があるものの，穀物生産は天候の影響を受けやすい構造となっている．パンパ地帯以外でも北西部のタバコ栽培，アンデス山脈地域の果樹栽培（メンドーサ州，サンファン州を中心としたブドウ栽培など），パタゴニア地方での羊等，農牧業はその地方の経済に重要な地位を占めている．

2）少雨温帯気候地帯

アルゼンチン国の気温と降水量によって区分した気候区分（図2）ごとの農業生産の状況は以下のとおりである．

アンデス山脈沿いの少雨温帯気候地帯は，北部は大部分がなだらかな高原となっており，北へ行くほど高度を増すため，緯度的に亜熱帯地域に入っても気温的には日較差が大きく，また日射量も多い．

しかし，降水量が200mm以下のため，潅漑なくしては作物栽培が不可能な土地である．したがって，将来潅漑施設が整備されれば優れた穀物栽培地域になる地域である．

表1．アルゼンチン国の土地利用．
（国際農林業協力会，1992による）
Table 1. Land Use of Argentina.

（単位：千 ha）

	1976	1981	1986	1991
総面積	276,689	276,689	276,689	276,689
陸地	273,669	273,669	273,669	273,669
農用地	170,800	170,300	169,800	169,300
耕地	25,000 F	25,000 F	25,000 F	25,000 F
永年作物用地	2,200 F	2,200 F	2,200 F	2,200 F
永年牧草地	143,600 F	143,100 F	142,600 F	142,100 F
森林	60,270	60,000 F	59,600 F	59,100 F
その他	42,599	43,369	44,269	45,269
潅漑面積	1,477	1,580 F	1,640 F	1,690 F

F：FAO 推定値

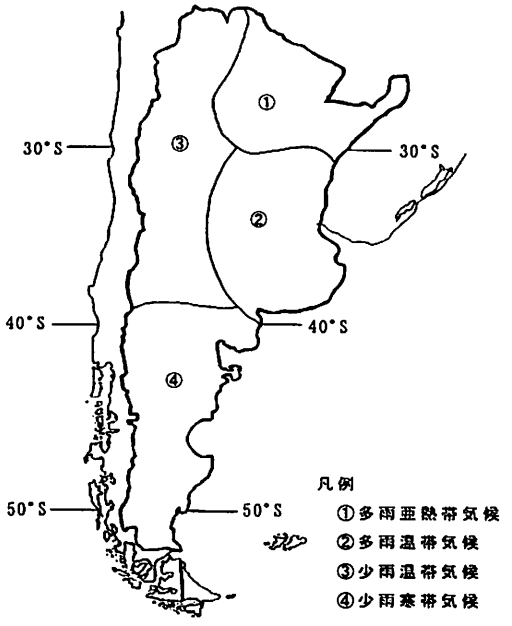

図2. アルゼンチン国の農業気象区分.
Fig. 2. Division of Agricultural Meteorology in Argentina.

この地域では強い日射量と日較差のある気温を利用し，古くはアンデス山脈の雪解け水，谷間の流水，多目的ダムの用水を利用した潅漑農業が行われ，メンドーサ，サン・ファンのブドウ（年産約350万t）とツクマン，サルタのサトウキビ（年産約1,500万t）が特産物として栽培されている．この他，タバコ，パンパ地帯と出荷期差を利用した野菜，柑橘類，あるいは一部谷間の降水量が多いところでのトウモロコシ，コウリャンの栽培も行われているが，ほとんどは潅木林とまばらに草の生えた自然のままの状態にあり，数ヘクタールに1頭程度の子取り用の肉牛の放牧が行われているに過ぎない．

3）農業生産の動向

①主要穀物

近年の穀物等の生産量は，小麦，トウモロコシ，大豆，ヒマワリを中心におおむね年間3～4千万tで推移（1990年：総作付面積1,912万ha，総生産量3,427万t，1991年：総作付面積1,881万ha，総生産量3,787万t）しており，1991年の主要穀物の生産量は，小麦940万t，トウモロコシ1,069.9万t，ソルガム620万t以上となっている．

②果　物

アルゼンチン国の代表的果物であるリンゴは，近年100万t生産されており，リオ・ネグロ，ネウケンおよびメンドーサの各州で全体の90％を占めている．1970年代には全体の1/3がブラジルなどに輸出されていたが，1980年代後半にはブラジルの国内生産力が増し，輸出は約20万tまで減少している．

ナシもリンゴと同様の地域で年間約20万t生産され，約2/3近くが輸出され，年間5,000万ドルの収入をあげている．

柑橘類は，レモンがツクマン州を中心に年間50万t，オレンジがエントレ・リオス，コリエンテスの2州を中心に年間約60万t生産されている．

またブドウは，毎年約30万haで約300万t生産され，メンドーサ州，サンファン州が全体の90％を占めている．

③野　菜

ジャガイモは，ブエノス・アイレス州を中心に約10万haで250万tが生産されている．トマトは全国（11州）で，特にブエノス・アイレス市などの大都市近郊は生食用が，またアンデス地方では加工用（ケチャップ用）が約3万haで約70万t生産されている．エンドウマメは青果市場用青エンドウと穀物用乾燥エンドウがあるが，栽培面積は両者とも約1万haで生産量は青エンドウが2.5万t，乾燥エンドウはその半分程度になっている．青エンドウは，フフイ，サンタ・フェ州，乾燥エンドウはブエノス・アイレス州が中心となっている．乾燥エンドウは数少ない輸出野菜で，ブラジルに毎年1～6千万t輸出している．

④畜　産

(1) 牛

牛は，パンパ地帯を中心に約5,300万頭が飼育されており，過去10年間の増加率は0.1％以下とほとんど変化がない．年間約1千万頭の屠殺により，牛肉が2～3百万t生産されており，このうち30数万tが輸出されている．輸出先は欧州，米国向けであるが，アルゼンチン国は口蹄疫の汚染地域となっており，日本には農林水産大臣が指定した13工場（1993.4.1現在）で加熱処理した牛肉のみ輸出されている．

国民一人あたりの牛肉の年間消費量は80～90kgで，最近の10年間の平均国内消費量は230万t/年，輸出量は37万t/年となっている．

4）潅漑の現状

アルゼンチン国の潅漑プロジェクトには，中央政府が担当するものと，州政府が担当するものとがある．前者は水・エネルギー省の所管であり，後者は公団方式か，州独自のものである．

アルゼンチン国の全潅漑面積は154万ha（1978）で，

耕地面積に対する潅漑農地の割合は43％である．潅漑はそのほとんどが北西部で行われている．

潅漑農地の主要作物は，サトウキビ，柑橘類，ワタ，タバコが，サルタ，フフイ，ツクマンの各州で，またアルファルファ，ブドウ，ナシ，野菜が主に，サン・ファン，メンドーサ，コルドバ，リオ・ネグロの各州で，さらにアルファルファ，リンゴ，野菜が主にチュブト州で作付けされている．これらは専ら畑地潅漑の方法によっている．

一方，水稲は水の豊かな低湿地で作られている．国の北東部にあたるアルゼンチン・メソポタミアがその作付地域で，パラナ川とウルグアイ川に挟まれる長さ約1,100km，幅200～380kmの肥沃な土地である．ミシオネス，コリエンテス，エントレリオス州の3州のうち，コリエンテス州がその中心で，州の大半はパラナ川の三角州の堆積原である．この地域での潅漑主作物は水稲，タバコ，柑橘類，牧草である．

一般畑地域では，潅漑組織の90％は地表の水路網でカバーされ，潅漑の方法は主に畦間法が用いられてきた．近年アルファルファなどに散水法が採用されている．水田地域では水盤法がとられている．

排水施設は本来潅漑施設と密接に協力して運営されるべきであり，アルゼンチンでは，多雨湿潤地，または河川下流の低湿地などに，排水を考えるべき地域が少なくない．その面積は潅漑面積の5倍以上にもなるとみられる．

その他，畑地潅漑のほとんどは年降水量が500mm以下の地域で行われ，土壌塩類の洗脱に必要な排水をもあわせて考えなければならない．

5）中南米地域の潅漑排水に関する農地劣化対策プロジェクト（1988～91）FAOの勧告

（プロジェクトの概要については本文末尾に附記）

(1) 潅漑による塩害を防止するのに必要な技術的対応（潅漑方法の選択，適切な潅漑水量，水質の吟味，効果的排水施設，塩分溶脱水の適時実施など）
を地域に応じて選択すること

(2) 土地所有，農産物価格，市場開拓など，農家の経済的社会的インセンティブを満足させる政策もきわめて大切である．

(3) 具体的には，農地劣化防止の技術指針・マニュアルとその内容普及のための研修，コンピュータによるGISの修得，活用による立体的な現状把握，総合的農業開発計画の樹立に着手すべきこと．

3．アルゼンチン国メンドーサ州の現状

メンドーサ州はアルゼンチンの西部に位置し，南緯30度にある．西はアンデス山脈によりチリと隔てられている．

降水量は年間200mm以下，総面積は15万km^2，人口は120万人である．また潅漑面積は36万haで，現在メンドーサ州はアルゼンチンで最も重要な潅漑地域である．

1）メンドーサ州の潅漑農業

アルゼンチンの潅漑農地の約30％がメンドーサ州にある（表2）．潅漑の伝統は1400年代からあり，最初のスペインの征服者が到来した1561年には原始的な5千haの潅漑農地があった．スペインの潅漑農業の伝統のおかげで，原始的なものよりもより組織化された植民地農業が起こった．また，近代的な地下水開発が今世紀の前四半世紀に鉄道およびヨーロッパからの入植者とともに開始された．

2）水　資　源

メンドーサ州の水資源はアンデス山脈を水源とし，地域を西から東に流れる5つの河川に依存している．これらの河川は，北から南に，メンドーサ川，トヌジャン川，ディアマンテ川，マラルゲ川，アトエル川である．農業に利用される河川水の量は186m^3/sである．また，メンドーサ州には18,000以上の井戸があり，地下水開発も非常に重要である．州全体で汲み上げられる地下水量は

表2　アルゼンチン国の州別潅漑面積．
(Consejo Foderal De Inversiones, 1970)
Table 2. Irrigated Area is various states of Argentines.

（単位：千 ha）

州名	潅漑面積	割合(%)
Mendoza	359.5	33.4
Satiago del Estero	125.0	11.6
Rio Negro	94.1	8.8
San Juan	93.6	8.7
Salta	93.2	8.6
Tucuman	82.4	7.6
Jujuy	63.5	5.9
Buenos Aires	43.5	4.0
Cordoba	39.0	3.6
Neuquen	31.5	2.9
Chubut	17.0	1.6
Catamarca	15.0	1.4
La Rioja	13.3	1.2
San Luis	5.5	0.5
La Panpa	2.2	0.2
合計	1,078	100

50m³/sにのぼる．

186 m³/sの水源が確保できるとした場合，年間の水量は587百万m³/sとなり，これをメンドーサ州の主要作物であるブドウの年間必要水量の7千m³/haで割れば，84万haが潅漑可能面積となる．しかし，実際には36万haしか潅漑されておらず，州の潅漑利用効率は約40％である．

現在のメンドーサ州の発展はオアシス経済により得られており，これにより人々は良好な生活水準を享受できている．これは，メンドーサ州においては非常にわずかな地表面で水資源と土地資源が利用されていることを意味する．

北部のオアシスは，メンドーサ川とトヌジャン川による20万ha以上の潅漑農地である．また，中央オアシスは地下水とディアマンテ川，アトエル川の2つの川による10万ha以上の潅漑農地である（図3，表3）．

また，メンドーサ州では昔から潅漑水の不足を地下水に依存しており，アルゼンチン国内の井戸の半分以上がメンドーサ州にある．平均的な井戸は直径10インチ，深さ250mとなっている．メンドーサ州における地下水による潅漑はメンドーサ市の北東約70kmに位置するサン・マルチン地区とマイプ地区が多く，それぞれ約19～16％の割合を占めている（表4）．

また，メンドーサ州における潅漑農地の規模は，0～5 haが一番多く約45％を占めるが，面積では約9％に過ぎない（表5）．

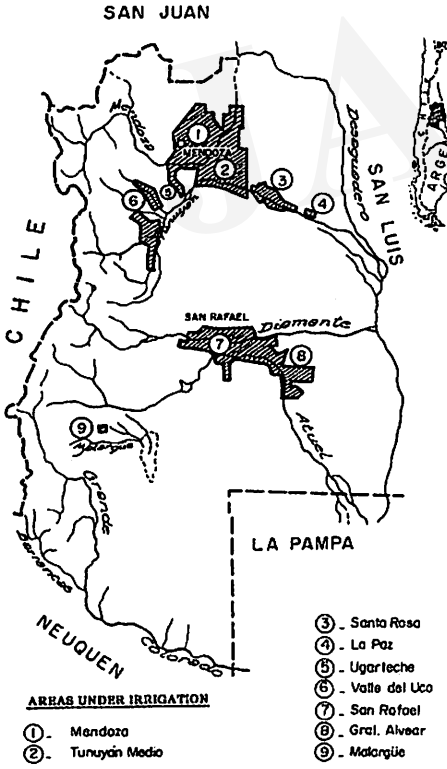

図3．メンドーサ州の潅漑農地．
Fig. 3. Irrigated Yield in Mendoza.

3）潅漑施設

メンドーサ州の各河川にはダムがあり，幹線用水路はライニングされている．現在，5つの河川におけるオアシスには8千kmの用水路と2千kmの排水路がある．ま

表3．メンドーサ州の潅漑面積と台帳登録面積．
(DGI Mendoza, 1995)
Table 3. Irrigated Area Registered Land Area in Mendoza State.

（単位：ha）

河川名	潅漑面積	台帳登録面積
Mendoza	81,682	91,877
Tunuyan	91,000	105,490
Diamante	68,841	92,397
Atuel	87,000	119,766
Malargue	1,000	5,372
Arroyos y Vertientes	30,000	67,993
Rio Colorado	---	72,650
合計	359,523	555,545

地下水による潅漑も含む．

表4．メンドーサ州の地下水潅漑の割合．
(DGI Mendoza, 1995)
Table 4. Groundwater Use Area Proportion in Mendoza.

（単位：％）

地区名	割合	地区名	割合	地区名	割合
Ciudad	0.1	San Martin	18.6	Tupungato	2.4
Las Hearas	2.7	Santa Rosa	6.1	San Carlos	3.7
Lavalle	8.0	La Paz	0.7	Tunuyan	4.1
Lujan	4.8	Rivadavia	7.2	計	10.2
Godoy Cruz	0.2	Junin	6.7		
Guaymallen	8.4	計	39.3	San Rafael	8.3
Maipu	15.6			Gral. Alvear	2.3
計	39.8			Malargue	0.1
				計	10.7

表5．メンドーサ州の潅漑規模別個所数および面積．
(Censo Nacional Agropecuario, 1988)
Table 5. Irrigation Area in Mendoza.

規模（ha）	個所数	面積（ha）
0 - 5	14,147	35,193
5.1 - 10	6,849	51,9115.5
10.1 - 25	6,721	109,172
25.1 - 50	2,755	98,169
50.1 - 10	1,271	90,168
計	31,743	384,514

たダム下流に設けられた水力発電所は州の電力需要をまかなうとともに，地下水のくみ上げにとって十分かつ安価な電力を供給している．

4）土　壌

潅漑農地の土壌は沖積性のものであり，主として砂質ロームである．土壌は深く肥沃であるが窒素分が欠乏している．ところによっては，地下水面が地表近くにあり，そのため塩類土壌が低地にしばしば出現する．

5）農　業

メンドーサ州の農業は，ブドウ，オリーブ，果物および野菜といった地中海的な生産モデルにならって発展した．この生産モデルはスペイン，イタリア，フランス，ドイツおよび他の地中海沿岸国からの入植者により導入されたものである．5つのオアシスにおける主要な栽培作物は，ブドウで231千haの面積を持つ．第2の作物は果物で，特にプルーン，オリーブ，モモで50千haの面積を持つ．次が野菜で，北のオアシスで栽培され，面積は30千haである．またその他の土地では飼料作物とポプラが植えられている．現在国内市場内の相互競争により農業生産の変化が起こっている．このため，南部のオアシスでは，潅漑草地での牛の肥育が奨励されている．メンドーサ州では年間1億ドルを近隣州からの牛肉の購入に支払っており，この取り組みによる成果が期待されている．また地域の農産物の輸出のための海外市場も求められている．

4．メンドーサ州の土壌劣化に対する取り組み

メンドーサ州における土壌劣化は，潅漑農地における塩類化が問題となっている．メンドーサ州の潅漑農地のうち塩類化している農地は，その58％の255,940haを占めている．メンドーサ州は潅漑面積で，アルゼンチン国の約30％を占めているが，塩類化の面積では約44％を占めており，アルゼンチン国内では相対的に塩類化が進んでいる州である．

1）潅漑農地の塩類化の原因

メンドーサ州における潅漑用水の水源は，河川水および地下水である．アンデス山脈を水源とする河川水の水質はもともと良好であるが，下流部ほど水質が悪化しており，現在河川の下流2/3の部分で農地における塩類集積が問題となっている．

この原因としては，

①メンドーサ州の土壌がそもそも海成土壌で塩分を多く含むため，潅漑により地中の塩分が地表部に上昇してくる．

②潅漑用水の管理が不適切なため，過剰な用水が潅漑されている．これは，この降水量の少ないメンドーサ州におけるオアシス農業の歴史として，古くからの農民の習慣で「潅水は多ければ多いほどよい」という意識によるもののようである．

例えば，

(1) トゥルマージャでは，800mm以上も余分に潅漑されている．

(2) 南部のアパドレでは，実際には4.5万haの農地しかないのに，12万ha分の用水が潅漑されている．

③潅漑用水が不足するため，農地の排水が用水として反復利用されており，上流部の農地からの塩分を含んだ排水が潅漑用水として利用されているところもある．

といった事が複合的に組み合わさっているようである．

また地下水は，河川水の用水路が届かないところ，農地開発の結果地下水しか利用できないところ，経済的に有利な作物（野菜など）を作付けしているところ等で利用されているが，そもそも浅い地下水は塩分を多く含む傾向にあるため，浅井戸の利用が塩類集積の原因となっているところもある．またこの様なところでは井戸を深くする（100～300m）といったことが行われているが，その深井戸に塩分を多く含んだ地下水がつながって水質が悪化するといった事も起こっている．さらに水質の良好な井戸に潅漑水が混入し，地下水の塩分濃度が高くなっているところもある．現在メンドーサ州における30％の井戸が塩分濃度が高いという事で問題になっている（特にサンタ・マリア地区では50％の井戸が問題となっている）．

さらに石油採掘時に石油と同時に汲み上げられる多量の塩水が，河川に排水されているという事もあり，現在その対策（① 塩水を地中に戻す，② 蒸発させる）が部分的にとられているものの，潅漑用水の水質悪化の一因にもなっている．

また，メンドーサ州では近年酒造，缶詰，皮革（なめし）等の約90の工場からの産業排水として，汚水（細菌，バクテリア，重金属）が潅漑用水路や農地内の排水路へ流入しており，メンドーサ市近郊では1～1.5m^3/sの汚水が潅漑用水に混入し，これが野菜栽培に利用されるなど，潅漑用水の水質悪化が農地への塩類集積問題にとどまらず，地域の社会問題・環境問題となっている．この問題に関しては，現在GTZがその対策を検討中であり，① 排水をすべて処理する．② 工場自体が規制して排水する．③ 用水の影響を受けないような農業（種